

AD-A012 658

METRA PRODUCIBILITY INVESTIGATION

R. C. Chapman, et al

Aeronutronic Ford Corporation

Prepared for:

Army Mobility Equipment Research and
Development Center

1 June 1975

DISTRIBUTED BY:

NTIS

National Technical Information Service
U. S. DEPARTMENT OF COMMERCE

AD A 012658

213094

WDL-TR5880
1 JUNE 1975

METRA PRODUCIBILITY INVESTIGATION

FINAL REPORT

Contract: DAAK02-75-C-0003

Prepared for:
U.S. ARMY MOBILITY EQUIPMENT
RESEARCH AND DEVELOPMENT CENTER
Fort Belvoir, Virginia

D D C
RECEIVED
JUL 23 1975
REGULATED
A



DISTRIBUTION STATEMENT A
Approved for public release;
Distribution Unlimited

Reproduced by
NATIONAL TECHNICAL
INFORMATION SERVICE
U.S. Department of Commerce
Springfield, VA. 22151

Aeronutronic
Aeronutronic Ford Corporation
Western Development Laboratories Division
3000 Fabrian Way
Palo Alto, California 94303

Report WDL - TR - 5880

METRA PRODUCIBILITY INVESTIGATION

Dr. R. C. Chapman
Israel Polidi
William DeHaven
Aeronutronic-Ford - Western Development Laboratories
3939 Fabian Way
Palo Alto, Calif. 94303

1 June 1975

Final Report Contract: DAAK02-75-C-0003

Prepared for:
U.S. ARMY MOBILITY EQUIPMENT
RESEARCH AND DEVELOPMENT CENTER
Fort Belvoir, Virginia

Summary

Normally linear components such as coaxial cable connectors in radio frequency systems actually are very slightly nonlinear. Sensitive systems can detect spurious signals produced by these nonlinearities and their operation can be impaired by them. This report offers some theoretical explanation of this phenomena as well as some practical methods of minimizing the nonlinear effects.

Two of the most predominant causes of nonlinear effects are electron tunneling through thin oxide layers separating the metallic conductors at conductor junctions and the semiconductor action created at a metal-oxide-metal interface. Basically the thickness of the oxide layer will determine whether tunneling or semiconductor action takes place. Contingent on fabrication processing, another potential source of nonlinear operation can be microdischarge between microcracks in metallic structures.

It has been determined that the important parameter in the generation of these low level spurious signals is the current density at conductor junctions. Therefore, the techniques for minimizing nonlinear effects, are in general, concerned with reducing current densities, reducing the number of junctions and improving the quality of the remaining junctions. A general step by step design method for minimizing system nonlinearities and resultant harmonic generation is presented in the following report.

TABLE OF CONTENTS

	<u>Title</u>	<u>Page</u>
1.	INTRODUCTION	6
2.	PHYSICAL MECHANISMS OF NONLINEARITIES	8
2.1	Contact Effects	8
2.2	Oxidation Processes	8
2.2.1	Oxide Damage and Regrowth	10
2.2.2	Time Effects	10
2.3	Physics of Nonlinearities	11
2.3.1	Electron Tunneling	14
2.3.2	Semiconductor Junction Action	15
2.3.3	Microdischarge	17
2.3.4	Extremely Low Level Mechanisms	18
3.	IDENTIFICATION OF PROBLEM AREAS	19
4.	PRODUCIBILITY CONCEPTS	26
4.1	General Guidelines	26
4.2	The Role of Current Density	26
4.3	Minimizing the Number of Transitions	28
4.4	Contactless Transitions	28
4.5	Effect of the Surface Smoothness	28
4.6	Effect of the Hardness of the Material	29
4.7	Effect of the Chemical Properties of the Metals	29
4.8	Effect of Soldering	29
5.	EXPERIMENTAL LINEARIZED HARDWARE	31
5.1	Test Fixtures	31
5.1.2	Filters	31
6.	PRODUCIBILITY DESIGN AS APPLIED DIRECTLY TO THE METRRA EQUIPMENT	42
6.1	Transmit Filter	42
6.2	Balun in the Transmitting Antenna	46
6.3	Antenna Coupling	47
6.4	Receiver Filter	48
6.5	Backpack Version	49
6.6	Combined Transmit Front End	49
6.7	Chassis Considerations	49
7.	CONCLUSIONS AND RECOMMENDATIONS	51
7.1	Data Translation	51
7.2	Source Identification	51
7.3	Brassboard Model Linearization	52
7.3.1	Transmit Filter	52
7.3.2	Receiver Filter	52
7.3.3	Antenna Isolation	52
7.4	Ruggedized Field Unit	52
7.5	Backpack Version	52

TABLE OF CONTENTS

(cont'd)

<u>Title</u>	<u>Page</u>
<u>Appendices</u>	
Appendix A: Relation between third order intremodulation products and third harmonic generated by the same device	54
Appendix B: Frequency Translation of experimental data	57
Appendix C: Calculation of the currents in a resonant cavity at a frequency far from resonance	60
Appendix D: Computation of the Radiated Power by a Contactless Cable Coupler	66
Appendix E: Test Procedure	69

List of Illustrations

<u>Figure</u>	<u>Illustration</u>	<u>Page</u>
1	Model of Two "Smooth" Metal Surfaces in Contact, Microscopic Scale...	11
2	Junction Contact Unit Model Circuit	12
3	The total load bearing area between two surfaces increases at a slower rate when the surface ripples are random in height.	13
4	I-V Characteristic of Metal-Oxide Metal Junction	13
5	Potential Barrier at Contact Between Two Metal Surfaces	14
6	NPN Metal-Oxide-Metal Junction - Zero Bias	16
7	Metal-Oxide-Metal Junction with Applied Bias	16
8	Areas in shaded box represent potential sources of third harmonic generation.	20
9	IM Product Experimental Data	21
10	Transmit Filter	22
11	Filter Cross Section in the Low Impedance Area	23
12	Coupler for the Cable Center Conductor	33
13	Standard Sleeves for Soldering on the Cable Jacket	33
14	Solderless insulated Coupler Shorted at the End by Clamps - $\frac{1}{2}$ Wavelength	34
15	Short Mechanical Coupler Solderless - Not Insulated	34
16	Solderless, Insulated Coupler Open Ended - $\frac{1}{4}$ Wavelength	35
17	Clamp	35
18	Internal Structure of Telonic Lowpass Filter	36
19	Internal Structure of Aeronutronic-Ford Filter Specially Constructed for Low Level Linearity	37
20	Insertion Loss - Aeronutronic Filter	38
21	Return Loss - Aeronutronic Filter	39
22	Skirt Characteristics - Aeronutronic Filter	40
23	Composite Characteristics - Aeronutronic Filter	41
24	Connection of the cable to the filter outer conductor. The supporting sleeve removes the stress from the soldering.	44
25	Balun	45
26	Band Reject Filter - Combined with Balun	46
27	Band Reject Filter - Combined with the Balun (Alternate Solution)	47

<u>Figure</u>	<u>Illustration</u>	<u>Page</u>
B-1	Equivalent Circuit of an "A" Spot Being Driven by a Generator	58
B-2	Frequency Response of the Transfer Function of the Network of Figure B-1	58
C-1	Cavity and Generator	61
C-2	Transmission Line Equivalent to the Resonant Cavity	61
C-3	Generator Capable of Delivering 200 Watts to a 50 ohm Load	62
C-4	Equivalent Cavity Circuit Used in the Example	62
D-1	Detail of Insulated Coupler	66
D-2	Model of Insulated Coupler	67
E-1	Test Setup - Transmitter-Receiver Coupling Measurement	74
E-2	Test Setup - Baseline	74
E-3	Test Setup - Filter	75
E-4	Test Setup - Test Fixtures	75
E-5	Cable Dimensions for Soldered Connectors	76
E-6	Preparation of Cable for Mechanical Couplers	77
E-7	Contactless (Intermediate Length) Mechanical Coupler	77
E-8	Assembled Cable and Coupler	78

1. Introduction

This study was undertaken to identify sources of nonlinear generation in the METRRA equipment, to indicate possible ways to alleviate the problems caused by nonlinearities, to suggest methods for producing the parts identified as most responsible for harmonic generation such that they will operate in a linear manner, to generate a set of rules for producibility of linear components and to apply these rules for the specific case of the METRRA equipment.

To be able to accomplish this task, it was necessary to use the results of past theoretical and experimental efforts at Aeronutronic-Ford WDL division done within the frame of other programs and continuing at present. Stable test facilities with the ability to test IM levels 210dB below the carriers and a source of information have been accrued. However, with all the valuable facts learned thus far, it must be remembered that the science of nonlinear product generation in passive components is still very new and there are still many unanswered questions. Every new study attempting to answer existing questions besides finding some answers, opens new areas to be explored and additional questions. For example, the data available at Aeronutronic-Ford WDL was taken on waveguide structures at X-Band. The METRRA utilized coaxial structures at lower frequencies. This generated the need for translating data from waveguide to coax and from one frequency to another. Similarly, the relation between two types of third order nonlinearities, third harmonic, and third order IM products had to be established. The rule for translation of the data for different power levels was derived previously. Thus the first steps in this study was theoretical and dealt with rules of data translation.

With the help of these rules and with some knowledge of the METRRA transceiver, the harmonic level was estimated quantitatively for the different system components. A list of all potential nonlinear sources was generated. Two particularly critical areas were identified; one in the transmitter output including antenna, balun and filter. The single component most responsible for the nonlinear generation was estimated to be the transmit filter so this component received considerably more attention than the others.

Next, the activity moved from identification and analysis to practical techniques for curing the problem. One "clean up" transmit filter was produced at WDL. Designed for linear operation, it was to prove the methods for reducing the nonlinearities and at the same time help establish a quiet test bed, which could then be used to test other components and gain new information needed for design of IM free components. Reports from Ft. Belvoir confirmed that this filter played an important role in better understanding and in establishing a quiet test bed.

With this problem solved it becomes possible to use the METRRA unit as a test setup for testing some producibility concepts and in this way to provide much needed information for the manufacturing of better components for eventual field equipment. Several test fixtures have been supplied by WDL. Some of these fixtures are to verify theoretical prediction of the effects of current density while others should provide some insight into linear methods of joining two coaxial cables. At the time of writing this report the test data is not available.

As mentioned before, other components contribute to nonlinear generation too. After quieting of the transmit side with sufficient linear filtering, it was found that the receiver filter was the next most nonlinear component. It also became apparent that if the antenna isolation is not sufficient the receiver filter will be hit with considerable power and this will cause IM generation. In essence, either the antenna has to provide good isolation or the receiver filter will have to be of special linear design.

General guidelines for producibility of the METRRA equipment were then made. Specific methods and means of alleviating the problems caused by the nonlinearities were the subject of the producibility design. Part of this effort was spent in resolving the most immediate problems. These solutions can help for the conditions of the lab but may have deteriorated performance in service in the field. A longer term solution is that of "ruggedized design" which entails the combining of individual components and in effect imposes the condition of linearity ahead of the other specifications. These ideas, it is realized, will be possible to use only in future designs, but it is believed they will present the ultimate of what is known in this field.

2. Physical Mechanisms of Nonlinearities

Nonlinearities in normally linear components can be caused by several different mechanisms. These mechanisms are believed to include nonlinear semiconductor effects, tunneling at metal to metal junctions, gaseous conduction phenomena, and water vapor absorption.

Semiconductor effects and tunneling contact junctions are discrete sources of nonlinearities. Contact generation is strongly dependent on the contact geometry, pressure, and physical condition.

Other effects can be classified as distributed. These effects include gaseous breakdown which can occur at small gaps in the RF conductor such as occur at an insufficiently tightened connector. Some of the distributed effects to be discussed, such as the analogous Luxembourg effect, are primarily applicable to waveguide or other RF conductors subjecting air or other gases to high electric fields.

2.1 Contact Effects

Microscopically all surfaces are highly irregular. In addition, most metallic surfaces have an oxide layer several angstroms thick on their surfaces. When contact is made between surfaces, rupture spots through the oxide coating are formed, work hardening and cold welding of the metals occur at some spots, very thin oxide layers separate the metals at some spots, and thick oxide or void regions are formed in other spots. The actual impedance at the contact is then determined by two factors: the current conduction through the finite number of discrete contact spots, and the displacement current through the oxide and void regions.

2.2 Oxidation Processes

On an initially unoxidized metallic surface the process of oxidation occurs when oxygen molecules strike the surface at random times and in random places. Those molecules with higher energies or which impinge on a higher energy area of the crystal dissociate and form islands of oxide a few angstroms thick. The rest of the impinging molecules rebound elastically from the surface. A classical model in which the gas molecules are treated as rigid spheres striking a rigid surface gives good agreement with test data. Increasing the partial

pressure of the oxygen or the temperature of the gas increases the frequency of collision with the surface. Increasing the temperature of the surface increases the proportion of striking molecules which are absorbed and the surface diffusion rate of oxide particles. Oxide islands which form on the surface are initially discontinuous but form continuous layers first by diffusing to higher energy sites and then rediffusing from there. Oxide thickness will be nonuniform because the higher energy sites will form oxide at a higher rate since more of the oxygen molecules which hit these areas will dissociate. At some oxide thickness, temperature, and partial pressure of oxygen, there will be an equilibrium between desorption and absorption of oxygen at the surface and diffusion of the metal into the oxide and oxygen into the metal. When this occurs, the oxide thickness at the lower energy areas will tend to equalize with those of the more mature high energy areas. Over long periods of time and for relatively thick oxide layers the difference in oxide thickness between high and low energy areas will diminish. Growth will continue at a much reduced rate as long as there is a source of oxygen.

To simplify the picture of oxidation, consider a clean, oxide free single metallic crystal which is exposed to an oxidizing environment. If the crystal is perfect, the formation of oxide will be random on the surface and will tend to be greatest at the edges where the energy is higher. A fully oxidized single crystal will have a uniformly thick oxide layer on the surfaces with slightly thicker oxide at the edges.

A single crystal with imperfections such as slip lines and dislocations will have more regions of high energy than a perfect crystal and consequently more sites for preferential oxide build-up.

Polycrystalline metals carry the above models to the final step. Grain boundaries have much higher surface free energy than other imperfections so they have even more preference for oxidation. When grain boundaries also are stepped up or down they have additional free energy and oxidize more readily than planar grain boundaries. This polycrystalline model, with thick oxide layers at the grain boundaries and other high surface energy sites and a fairly uniform oxide thickness elsewhere most nearly agrees with actual conditions.

Oxide layers need not grow as a uniform planar layer. Under proper conditions

of temperature, pressure and concentration the oxide can grow as whiskers. The whisker form may be rods, ribbons, needles, hexagonal crystals, feathers or spheres. Shape also depends upon growth conditions. Whiskers grow from the base. Whiskers may act as punches, forcing their way through the oxide layers on mating surfaces when pressure is applied.

2.2.1 Oxide Damage and Regrowth

Consider two relatively smooth surfaces with oxide layers 50 to 80 angstroms thick. When contact pressure is applied the oxide on contacting peaks will first crack and then rupture. Cracking of the oxide may precede or follow deformation of the underlying metal, depending upon the relative compressive strengths of the oxide and the metal, the direction of the load and local temperature rises caused by pressure and rubbing friction. The result of oxide cracking is metal to metal contact with broken oxide particles in the interface. If the contact pressure is great enough or is accompanied by high rubbing friction, the two surfaces will actually weld, forming a metallurgical joint. More likely, however, is intermittent metallic contact with oxide particles trapped in the interface.

Increasing the surface roughness will decrease the number of contact points but may actually increase the number of metal to metal bonds because local peaks would tend to be sharper, more easily deformed, smaller in area and be subject to higher stresses. Higher stresses and greater deformation will give more surface-to-surface welding at equivalent contact pressures.

2.2.2 Time Effects

Once the oxide layers are broken, reoxidation will occur along the contacting surfaces except where welding has occurred. The amount and rate of reoxidation depends upon local partial pressure of oxygen, the nature and extent of surface-to-surface contact, temperature and contact pressure. The outer edges of the surfaces reoxidize first. Oxidation then progresses inward along the path of fewest contact points. The first reoxidation should occur within less than a day and there should be significant oxide film on the exposed surfaces within one or two days. The only hinderances to reoxidation of the contacting surfaces would be the exclusion of oxygen or surface-to-surface welding to form metallurgical bonds. Actual electrical contact degeneration will then depend upon the original number of welded spots and the initial contact formation. Even

for a large density of cold welded contact spots, the effects of mechanical stresses and deformation will eventually allow reoxidation of the spots and contact degradation will occur.

Oxidation rates can increase if the surface temperature is raised or if additional driving energy for diffusion is supplied. One type of driving energy that could be imposed is an electrical field which enhances oxygen flow into the lattice and metal ion flow toward the surface. Alternating fields create driving forces which first aid oxygen diffusion, then metal ion diffusion. This tends to distribute the oxygen more uniformly and deeper into the surface of the metal than in the absence of a field.

2.3 Physics of Nonlinearities

The nonlinearity of a contact will depend on the relative proportion of the conductance and displacement currents and the nonlinearity of the specific conduction mechanisms. Even optically ground surfaces have more irregularities than flat areas. Figure 1 illustrates the microscopic conditions at a metal-to-metal junction.

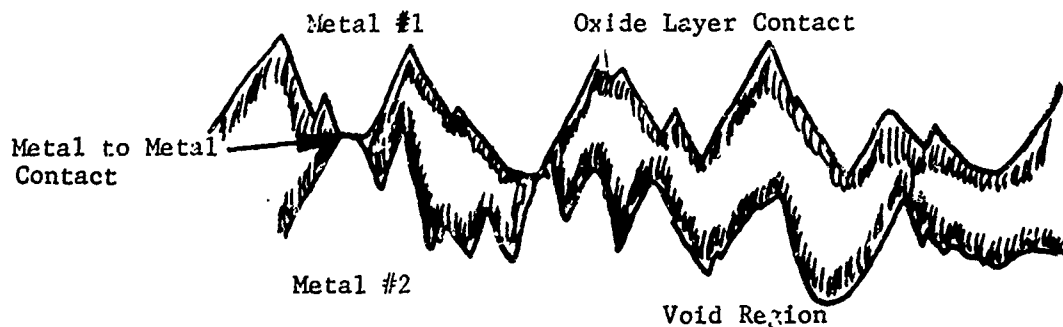


Figure 1

Model of Two "Smooth" Metal Surfaces in Contact, Microscopic Scale

The number of actual contacting points on any pair of surfaces is given by a statistical distribution of the number and height of peaks and the probability that there will be matching peaks and valleys or matching peaks and peaks. Increasing pressure will increase the surface contact area and the number of individual contacting points by deforming the metal and causing plastic flow.

The higher thinner peaks will deform first with low smooth peaks and valleys deforming last, if at all.

The equivalent circuit for one contacting spot, or A-spot as they have been called in the literature, is shown in Figure 2.

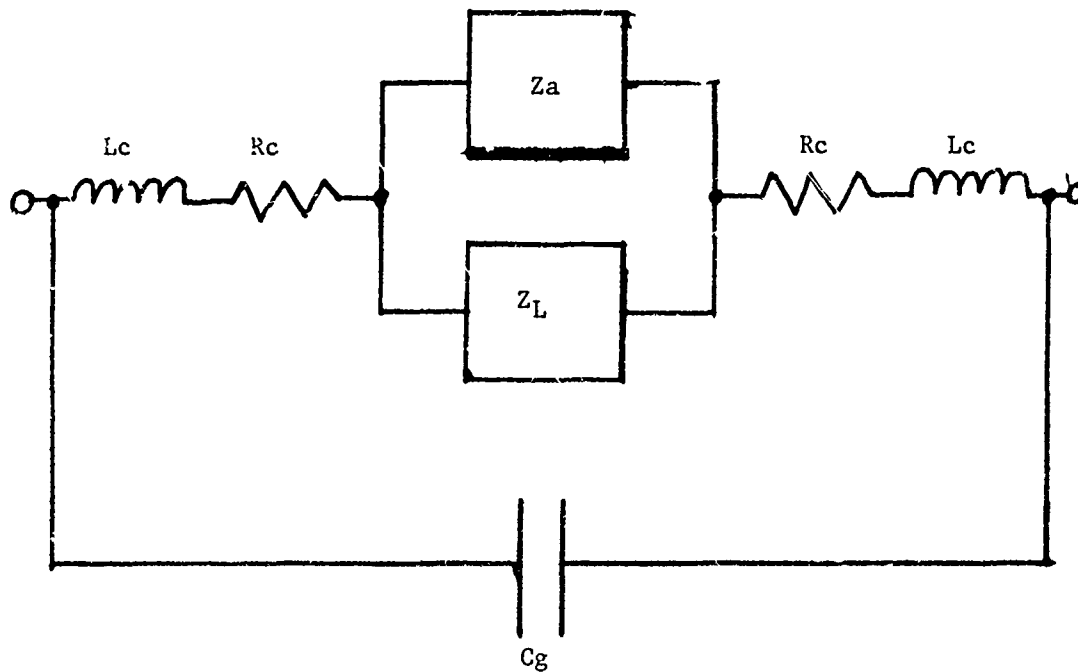


Figure 2

Junction Contact Unit Model Circuit

The inductance L_C is due to the narrow conducting peak and is called the constriction inductance; the resistance R_C is the constriction resistance; C_G is the capacitance due to the void or oxide filled regions surrounding the contacting peaks; and Z_A and Z_L are the impedances at the contacting points where the oxide layer is less than 5 angstroms or greater than 5 angstroms, respectively. Z_A and Z_L are believed to contain the nonlinear resistances.

The total load bearing area is increased with the applied pressure. If all ripples on the metal surface were equal in height, the increase would be proportional to the increase of the total load bearing area. However, since the ripples are random in height, when the pressure is increased new contacts will be made so that the total area of the load bearing spots will increase at

a reduced rate. Figure 3 illustrates this idea.

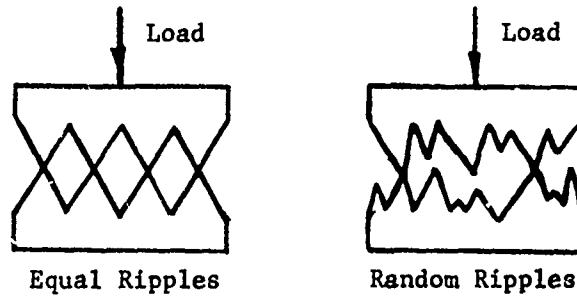


Figure 3. The total load bearing area between two surfaces increases at a slower rate when the surface ripples (due to surface roughness) are random in height.

The density of the contact spots and thus the density of the unit equivalent circuits will increase with the pressure. This will lead to the series of I-V characteristics illustrated in Figure 4.

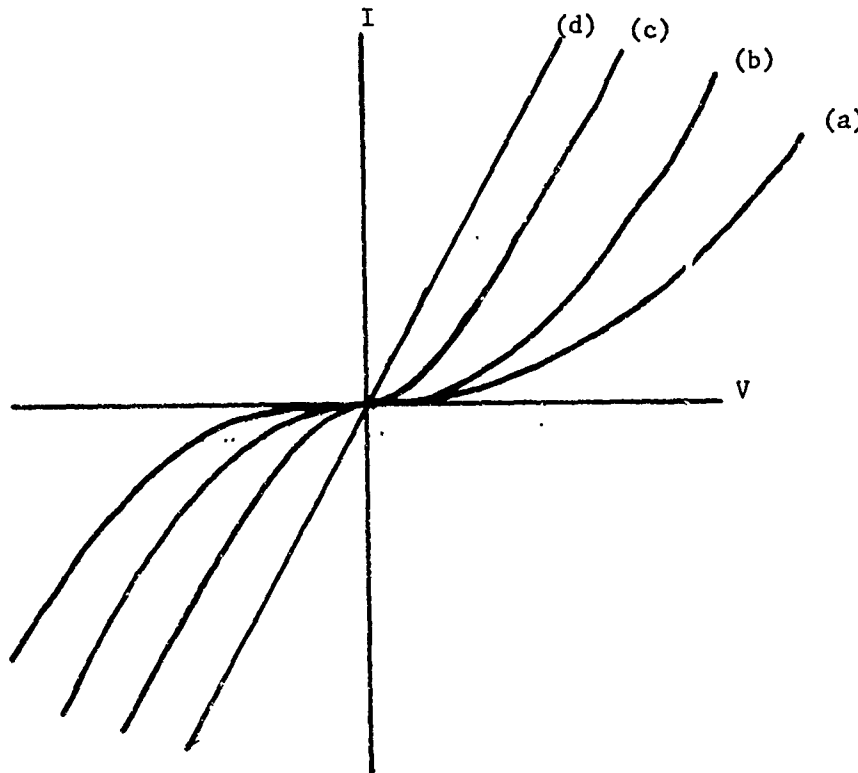


Figure 4

I-V Characteristic of Metal-Oxide-Metal Junction

Assuming that the load bearing contact contains a nonlinear element, a possible current for a light contact with few contact points is given by curve (a). With

increasing contact pressure more new contact points will be created, resulting in response curves (b) and (c). In the limit, the straight line (d) will be approached, which is the I-V curve determined by the external circuit.

2.3.1 Electron Tunneling

Nonlinear current conduction can occur due to electron tunneling through thin metal oxide films. This is a result of the wave characteristics of the electron which becomes pronounced in microscopic current conduction through thin monoatomic films. Such structures can be very nonlinear. Electron tunneling does not occur throughout the entire metal oxide layer but only in the small contacting A-spots where the oxide layer is less than approximately 50 angstroms thick. The situation at the A-spot is illustrated in Figure 5.

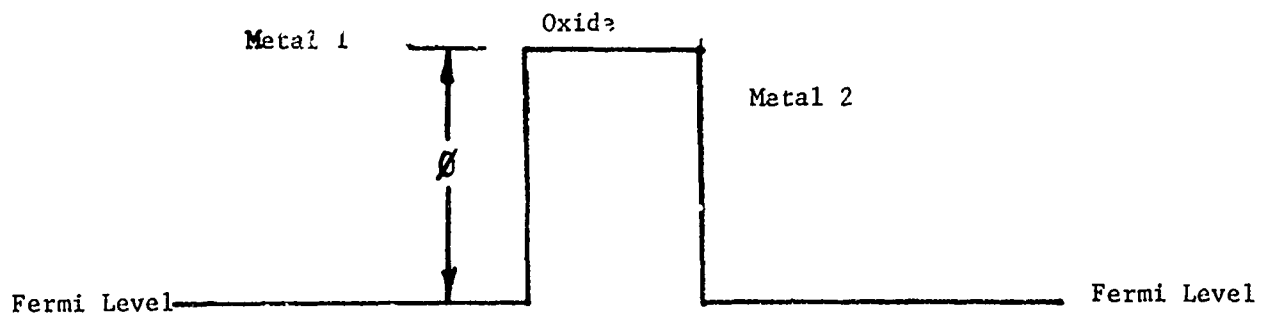


Figure 5

Potential Barrier at Contact Between Two Metal Surfaces

At the surface of the metals there is a potential barrier, ϕ , equal to the difference in work functions between the metal and the oxide. Due to the wave nature of the electron, there is a finite probability that it can move from metal 1 to metal 2 (or vice versa) even when its kinetic energy is less than ϕ . The probability of tunneling through the potential barrier between the energy wells is dependent on the potential barrier height and width and upon the energy of the particle in relation to the height of the barrier. The impedance presented to the tunneling current is slightly nonlinear. Theoretically calculated levels for third order intermodulation products are -140 dB for 200 watts or -87 dBm. As explained in Appendix I, this is also equivalent to a third harmonic level of -87 dBm. Higa¹ has discussed the case of electron

¹W. H. Higa, "Spurious Signals Generated by Electron Tunneling on Large Reflector Antennas." Proceedings of the IEEE, Vol. 63, Feb. 1975, pp 306-

tunneling in aluminum-aluminum oxide-aluminum junctions on the Deep Space Network giant antennas. He also discusses an experimental test fixture using aluminum foil contacts to demonstrate the nonlinearity of the junction.

2.3.2 Semiconductor Junction Action

Semiconductor junction action is another possible source for nonlinearities. A metal-oxide-metal contact can act as a rectifying device. For instance, the copper-copper oxide-copper junction has been studied extensively. The copper oxide acts basically as a P type semiconductor except right at the copper and oxide interface where, due to an excess of copper impurity atoms the oxide has an n characteristic. Because the work function of the copper oxide is larger than the work function of the copper, the copper-copper oxide forms an ohmic contact. The copper-copper oxide rectifier forms two p-n diodes back to back, or an npn transistor. Figure 6 is a schematic representation of the conduction band energy level of the structure with no applied bias. Figure 7 shows the situation when a bias is applied. The left hand junction is forward biased and injecting electrons into the p region where they diffuse to the other depletion region and are swept across the junction. If the bias is sufficiently large, the depletion region under reverse bias will widen until it reaches the other depletion region, the condition known as punch through. The region where current is controlled by diffusion disappears and all current becomes a drift current under an electric field. Because the charge injected into the p region is not neutralized by a corresponding charge of the opposite sign as normally happens through the base lead of a transistor, the current becomes space charge limited with a nonlinear I-V characteristic.

The same condition of punch through is reached if, instead of increasing the applied voltage, the thickness of the oxide layer is decreased until the two depletion regions meet. This is exactly the situation when the oxide layer is less than about 100 angstroms thick.

For oxides of copper less than 10\AA the tunneling nonlinearity will be the dominant source of unwanted signals. For film thicknesses between about 10 to 50\AA , both mechanisms are present and the distortion levels can be considered to be within 3 dB of those produced by the tunneling mechanism alone.

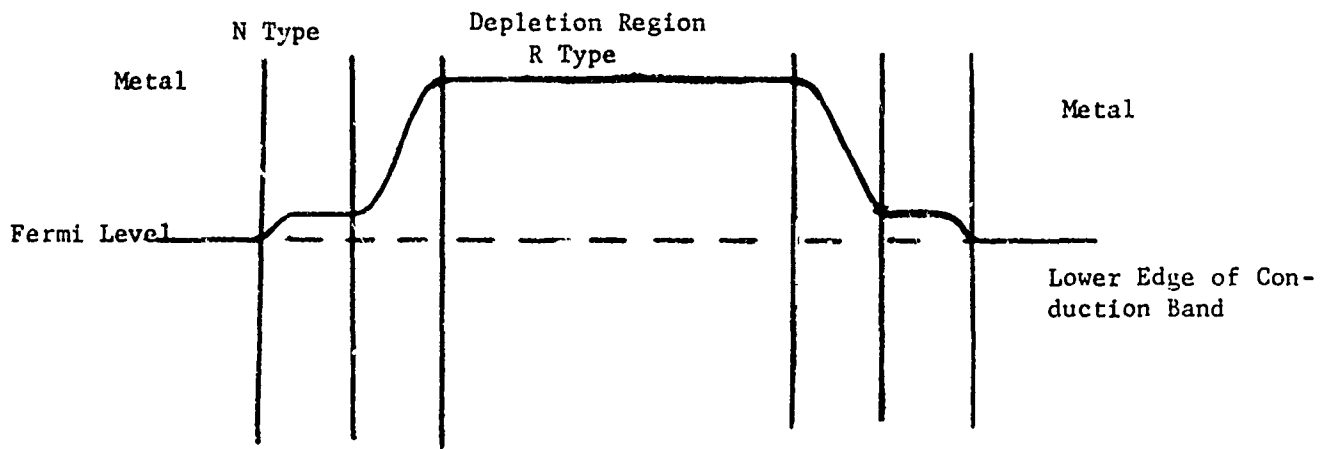


Figure 6

NPN Metal-Oxide-Metal Junction - Zero Bias

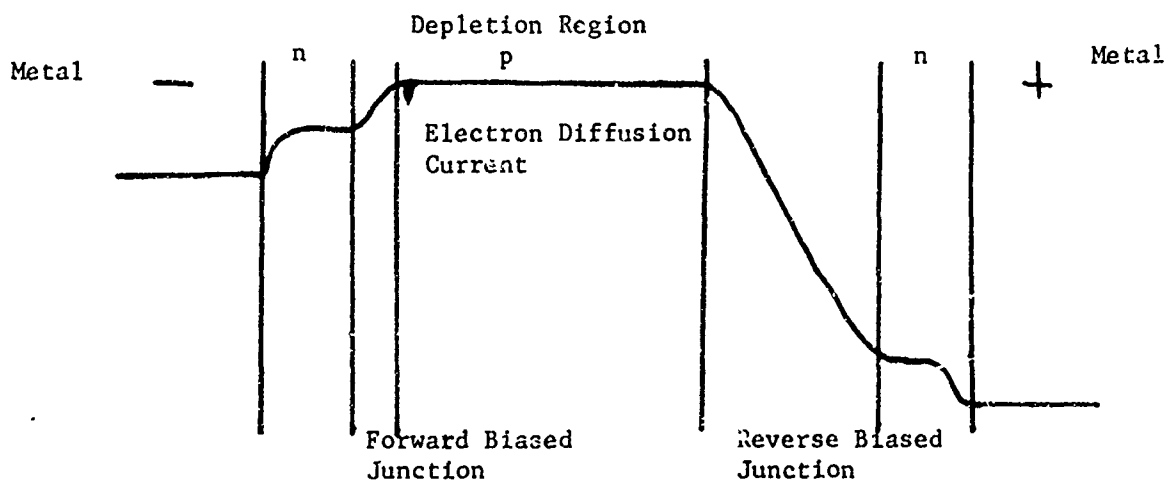


Figure 7

Metal-Oxide-Metal Junction with Applied Bias Voltage

2.3.3 Microdischarge

Experiments conducted both at WDL and at Stanford Research Institute have indicated that one of the most important nonlinear effects which can occur in metal to metal contacts is that of microdischarge, that is, the breakdown of microscopic regions of gas trapped between conductors. Microdischarge can occur even for contacts under sufficient pressure to ensure a reliable electrical connection. As discussed in the section on surface contacts, even two smooth contacting surfaces are rough on a microscopic scale and will include contacting peaks and noncontacting valleys. Microscopically the actual contacts may be made up of metal-metal oxide point contacts, thin filaments, impurities, suspended particles and shunt void regions. The total RF current flow then becomes the summation of microscopic RF tunneling currents, shunt displacement currents and parallel discharge currents between the whiskers and particles as the micro-contacts experience breakdown. Contingent on the actual microgeometry, the discharge phenomena can be the predominant mechanism.

Experience at WDL has indicated that surface treatment and coating in many cases can greatly influence the resultant IM generation level from microwave components. Additionally, for most contacts the IM level does not appear to be critically dependent on the actual contact pressure.

Both of these observations tend to support microdischarge as one of the more predominant generating mechanisms in that it is not as subject to contact pressure and is highly dependent on the actual surface micro-geometry, presence of impurities and whiskers, all of which can be influenced by surface treatment and coatings.

2.3.4 Extremely Low Level Mechanisms

Tunneling, semiconductor junction action and microdischarge are believed to be major contributors to nonlinearities in normally linear components. The following discussion on extremely low level effects is included mainly for completeness. These effects are the "analogous Luxembourg" effect and water vapor absorption.

In the analogous Luxembourg effect, a strong signal in a waveguide modulates the electron collision frequency such that the attenuation characteristics of the medium encountered by a low power signal are significantly modified. A periodic modulation of the low power signal by a process which is inherently nonlinear results in the generation of a family of intermodulation products. A level of -160 dBm is predicted for a 6 KW carrier and a 3 KW carrier.

Water vapor in a waveguide structure constitutes a potential source of nonlinearity due to the absorption characteristics centered at 24 GHz which is dependent on the incident power level and water content. With a 6 KW carrier an IM of -132 dBm is predicted in a 10 meter waveguide run.

3.

Identification of Problem Areas

Since the level of nonlinear distortion is proportional to the current density, the most likely problem areas in the METRRA equipment are those with the highest current densities. These areas are associated with the transmitter power amplifier, filters, transmission lines, balun and antenna, and of particular importance, the junctions between these components. Figure 8 is a schematic representation of the problem areas.

The output power of the amplifier is 2KW (+63dBm) and the third harmonic produced by the tube nonlinearity is about 50dBm below the carrier. The cavity terminates with an SMA connector which is treated as a cylindrical structure propagating in TEM mode in the following calculations. The inner diameter of the outer conductor is 0.142 inches (.361 cm) and the outer diameter of the inner conductor is 0.050 inches (.127 cm). Since the impedance is 50 ohms we have a current

$$I = \sqrt{\frac{P}{Z_0}} = \sqrt{\frac{2000}{50}} = 6.32 \text{ amperes.}$$

The circumferences of the inner and outer conductors respectively are:

$$C_i = \pi d = 3.14 \times .127 = .399 \text{ cm}$$

$$C_o = \pi D = 3.14 \times .361 = 1.134 \text{ cm}$$

The line current densities on the inner and outer conductors are then:

$$J_i = \frac{I}{C_i} = \frac{6.32}{.399} = 15.81 \text{ A/cm}$$

$$J_o = \frac{I}{C_o} = \frac{6.32}{1.134} = 5.58 \text{ A/cm}$$

By using the data obtained on a previous program we can predict a distortion level for the above current densities. The graph in Figure 9 represents the data taken at Ford in a previous intermodulation study. This data is for the two carrier case in which the power of a carrier at 7.90 GHz is three times the power of a carrier at 8.05 GHz. As explained in Appendices A and B, the theoretical difference in levels between this two carrier third order intermodulation case and the one carrier third harmonic case is negligible. Therefore, this data can be used directly. A level of -90dBm has been observed in WR137 waveguide at a power level of 2kW and this level was observed to increase at a rate of 2.5dB for each dB increase in power level.

Using the current density of the inner conductor since it is three times that in the outer conductor the expected level of third harmonic is obtained in the following steps:

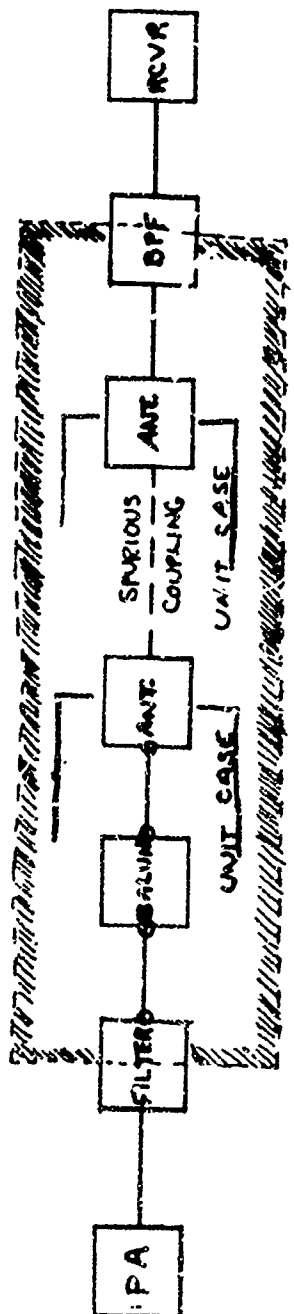


Figure 8

Areas in Shaded Box Represent Potential Sources of Third Harmonic Generation

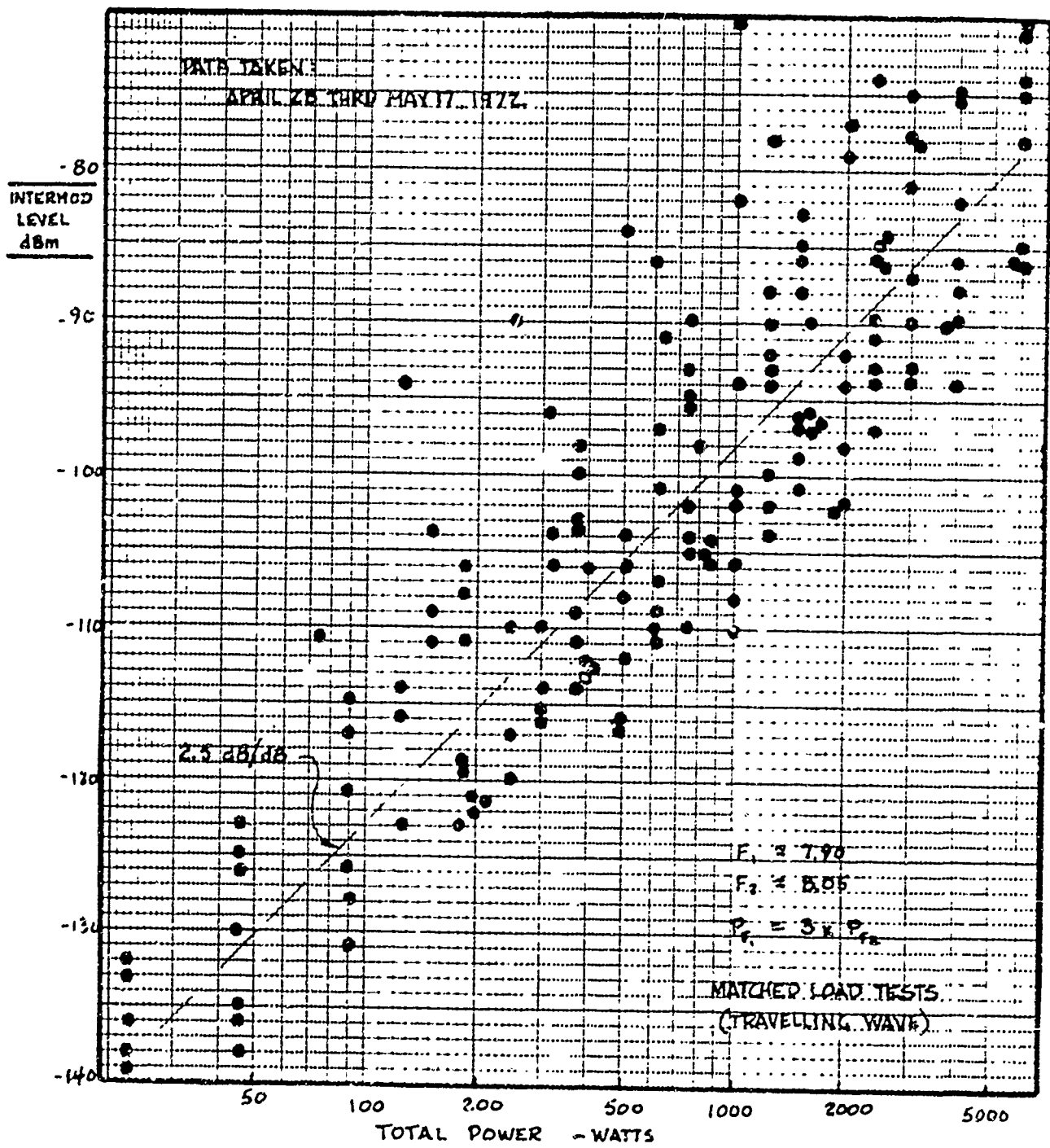


FIGURE 9
COLLECTION MATCHED LOAD DATA

The current density in a waveguide propagating in the TE₁₀ mode is given by

$$J_z = \frac{4}{\pi} \sqrt{\frac{W}{ab Z_{TE10}}}$$

where a and b are the waveguide dimensions, W is the power, and Z_{TE10} is the impedance presented to the TE₁₀ mode.

This formula reduces to

$$J_z = 2.6 \times 10^{-2} \sqrt{W}$$

for WR 137 waveguide and at a power of 2KW

$$J_z = 1.01 \text{ A/cm}$$

Therefore, the third harmonic level for our case should be

$$-90 + 2.5 \times 20 \log \frac{15.81}{1.01} = -60\text{dBm}$$

where the factor 2.5 comes from the 2.5dB/dB slope mentioned previously.

Obviously -60dBm can be neglected when compared to the +13dBm produced by the tube itself. This fact implies that there is no need for special treatment or design from the power amplifier stage to the input of the lowpass filter.

The Telonic lowpass filter in the equipment needs consideration. This analysis does not question the filter design and assumes that the filter is properly rejecting the third harmonic existing at its input. However, the filter may produce its own nonlinearities due to the internal structure.

The filter construction is shown in Figure 10. It is a nonresonant structure in which the impedance changes alternately from high to low along the line. Correspondingly, the current alternates from low to high, keeping the power level constant. First, we estimate the impedance levels in the filter. Approximating each section as a transmission line, we have for the low impedance large diameter section:

$$Z_{LOW} = \frac{60}{\sqrt{\epsilon}} \ln \frac{D}{d} = \frac{60}{2} \ln \frac{0.580}{0.522} = 5 \text{ ohms}$$

where D and d are defined in Figure 11 and $\epsilon = 2$ is the dielectric constant of teflon.

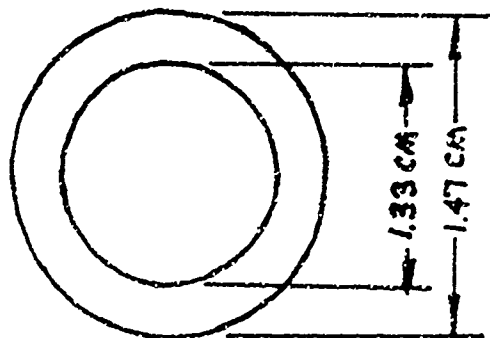


Figure 11. Filter Cross Section in the Low Impedance Area

The high impedance is computed in the same way assuming the coiled wire is acting as a helical coaxial cable.

$$Z_{\text{HIGH}} = \frac{60}{\sqrt{2}} \ln \frac{0.0500}{0.035} = 170 \text{ ohms}$$

The current in the low impedance section is:

$$P = I^2 Z \text{ or } I = \sqrt{\frac{P}{Z}}$$

$$I_{\text{LOW}} Z = \frac{2000}{5} = 20 \text{ AMP}$$

and in the high impedance is $I = \frac{2000}{170} = 3.43 \text{ Amp}$

The circumferences are:

$$C_o = \pi D = 3.14 \times 1.47 = 4.63 \text{ cm for the outer conductor}$$

$$C_i = \pi d = 3.14 \times .089 = .28 \text{ cm for the inner conductor}$$

and the current densities are:

$$J_o = \frac{I}{C_o} = \frac{20}{4.63} = 4.32 \text{ A/cm}$$

$$J_i = \frac{I}{C_i} = \frac{3.43}{.28} = 12.28 \text{ A/cm}$$

The increase in the harmonic generation, then is:

$$2.5 \times 20 \times \log \frac{4.32}{1.01} = 31.8 \text{ dB for the outer conductor and}$$

$$2.5 \times 20 \times \log \frac{12.28}{1.01} = 54.6 \text{ dB for the inner conductor.}$$

Then the most probable third harmonic level could be $-90 + 54 = -36 \text{ dBm}$, using only the calculation for the inner conductor since it is about two orders of magnitude larger.

The Telonic filter has a center output conductor comparable in size to the pin of the SMA connector on the power amplifier cavity and this in turn is comparable in size to the center conductor of the semirigid .141 inch diameter coaxial cable. All joints are soldered and conduct the same power. Therefore, the harmonic level should be the same as calculated for the SMA connector on the cavity or about -61 dBm . Spurious signals generated near the end of the filter are not attenuated and can propagate in only one direction - toward the antenna.

The connections of the balun to the filter and the antenna are also critical since they too are in spots where the spurious signals are unattenuated by filters before reaching the antenna. So, of all the component interconnections in the system the ones between the output of the filter and coax, between the coax and the balun and between the balun and the antenna are the most critical.

Because of the antenna isolation, the fundamental power incident upon the receive filter is considerably reduced from that in the transmitter. However, the receiver bandpass filter is a resonant structure, giving rise to higher circulating currents than would appear in a nonresonant type of filter. Any harmonics generated at the input of the filter travel essentially unattenuated directly into the receiver.

Metal to metal contacts in the areas of the equipment housing which will be illuminated by the antenna must be avoided. Single piece construction in these areas should be the design goal. More will be said about the equipment housing, filters and interconnects in sections 5 and 6 of this report.

To summarize, based on the idea that large current density means high potential for nonlinearities, the following list identifies the components we believe to be the most critical.

- Resonant cavity output connector
- Interconnecting cable
- Filter input connector
- Low pass filter
- Filter output connector
- Transition cable to balun
- Transmit antenna feed connections and cable
- Transmitting antenna
- Receive antenna
- Receive antenna
- Receive antenna feed connections and cable
- Receiver transition balun to cable
- Receive filter input section
- Case and peripheral structure

4. Producibility Concepts

In this section the concepts of producibility are treated in a general manner, closely related to the theory. The prime goal here is to gather a number of ground rules describing which techniques can be desirable and the reasons why they are desirable. These rules are general and for this reason can be applied to the METRRA equipment and to any other equipment as well. The specific application to the hardware of the METRRA equipment is discussed separately in one of the following sections.

4.1 General Guidelines

Briefly, and in order of importance, the guidelines and rules for producibility are:

4.1.1 Design the system to limit the nonlinear generating sources to as small a region as possible; that is, placement of clean-up filters as close to the radiating or receiving portions as possible.

4.1.2 Minimize the use of high Q resonant circuits in the resultant generating region. For example, use hybrid filter designs, bandpass or band reject filters rather than bandpass filters.

4.1.3 Eliminate as many mechanical contacts as possible in the generating region.

4.1.4 Increase the dimensions of transmission lines and resonator components to reduce the RF current density.

4.1.5 Use extreme care in the design of mechanical components. For example, use uni-body monolithic designs, lapped surfaces, welded contacts or contacts under pressure above the Young's modules.

These steps for linearized component design should be performed in the order given, that is, each design measure should be exercised, one by one, until sufficient linearity is reached to assure that the passive nonlinear harmonic generation is below the desired level. As can be observed, each step becomes progressively more difficult and involves more careful and costly design. More detailed discussion of each area is given in the following sections.

4.2 The Role of Current Density

Theoretical and experimental work at Aeronutronic-Ford WDL division indicate that a simple way of looking at the nonlinear generation in normally passive and linear devices is to assess the current density through this device. If there is a junction through which a current is flowing, there will be nonlinear products. The larger the current density, the larger the nonlinear products generated. From this statement we derive the following simple rules:

4.2.1 Wherever possible reduce the current density by increasing the size of the component.

This rule can be successfully applied to coaxial structures or where TEM mode of propagation exists. It should be possible, at least in some cases, to replace small size cables, coaxial filters, microstrip lines etc. with larger sizes of the same type components. This rule is not applicable to waveguide components since their size is determined by frequency requirements.

4.2.2 Wherever possible use impedance higher than 50 ohms.

Most of the components in the RF industry are standardized to the impedance of 50 ohms. However, there are components used at higher impedance like 75 ohm, 93 ohm etc. and standard cables are available at these characteristic impedances. Other components as filters or striplines can be fabricated at any impedance level (within reasonable limits). The power being transported can be made to have less current (and more voltage) by selecting a high impedance level. Physical size must be at least as large as would have been used in a 50 ohm system.

4.2.3 Avoid resonance effects.

Resonance effects are widely used in filters and periodic structures. Energy usually is stored in electric or magnetic fields and keeps transforming from one to the other. As a result of this, there are places where large currents will flow even for moderate or low power. The larger the capability to store energy, the larger will be the currents. The Q factor is the measure of the capability of the circuit to store energy. Then if a circuit can be built with a nonresonant structure, this structure should be preferred. But if it is necessary to use resonance, care must be taken to keep the Q factor low.

4.2.4 Provide parallel paths for the signal.

This rule will have very limited application and is advised only as a last resort. If every conceivable means of reducing the current density has been tried and still better results are needed then the signal can be split into two or more parallel paths. Cables can operate in parallel. If a transmitter followed by filter must drive an antenna array, the transmitter power can be directed through separate filters to drive different elements of the antenna array, thus reducing the current through each separate filter. It is realized that this solution is more expensive and is not easy; and, as indicated, is advisable only in a desperate situation.

4.3 Minimizing the Number of Transitions by Combining Several Units in One

In standard practice every component is designed separately and then all are integrated to form the final instrument. Due to this practice, every component has input and output junctions and any junction can become a generator of nonlinear products. The designer concerned with avoiding nonlinearities must ask the question whether it is possible to eliminate some of the junctions by combining the individual components. Undoubtedly, in many cases this will be simply impossible. In others, when using lots of ingenuity and creativity, this will be possible and will be a step in the right direction.

4.4 Contactless Transitions

In some special applications, the operation of an electrical connector can be simulated reasonably well by a capacitive contactless connection. Various configurations had been used more than ten years ago at Aeronutronic-Ford, the most popular of which is the configuration of two cylinders, one inside the other, separated by teflon and producing a large capacitor. Obviously a device like this has limitations in frequency response and cannot always be used. But at limited frequency band, the problem of response is not objectionable and then the contactless transition can be used. There is no test data to support the claim, but it is strongly believed that this type of transition must be the closest to the ideal in regard to IM or nonlinear generation.

The big disadvantage of this solution is that the transition must be relatively large. This makes its application limited to heavy, stationary equipment. Also, there may be a problem of RF leakage (see appendix D).

4.5 Effect of the Surface Smoothness

Any connector, flange or other component machined to a certain precision and depending on the quality of the fabrication can have some roughness of the surface. When two surfaces like this are brought together to produce an electrical contact, this contact is realized only at a relatively few spots rather than with the entire area. When the material is machined to a smoother surface, the number of contacts increases. Polished surfaces have been proven to produce less nonlinear products and, when possible, it is advised. In addition, careful surface preparation in terms of cleaning and subsequent coating has been found to be highly influential in the prevention of nonlinear generation. Remember, however, that a combination of smooth surface and high contact pressure is required to insure that the oxide layer is penetrated and reliable contact made.

4.6 Effect of the Hardness of the Material

Hard material will produce more nonlinear generation than soft materials. This statement can be explained by the effects of the surface smoothness by remembering that when two surfaces produce an electrical contact there is pressure applied on the surfaces. The pressure deforms the point contacts and causes more points to touch. However, while soft material can deform, causing the sharp peaks to give and producing a larger contact area, the hard materials deform much less and the contact occurs at only a few points. Thus a connector of stainless steel is likely to produce more harmonics or intermodulation products than brass, for example. There are some drawbacks that must be taken into account when considering this effect. Depending on the amount of pressure applied, every material will experience some deformation. For pressures obtained in tightening bolts, the hard materials will have elastic deformations while the soft materials will exhibit permanent deformation. If the material suffers permanent deformation it cannot be successfully used again. At Aeronutronics-Ford, waveguide flanges have been used together with soft copper gaskets, obtaining good results; but it was possible to use the gasket only once. Attempts at using a gasket a second time proved that the low nonlinear generation properties are lost. Gold plating has been used as soft gasket and when used only once gives good results. After that, the deformation of the material, scratches and similar effects can cause deterioration of the performance.

4.7 Effects of the Chemical Properties of the Metals

The metals of components conducting current are selected to have good conductivity or light weight. Three most widely used metals, silver, copper and aluminum, have excellent conductivity and the aluminum is lightweight. But all of them produce oxides on their surface and oxides play an important part in the nonlinear product generation process by tunneling and semiconductor action. Metals not producing oxides are highly recommended. Gold is particularly appropriate because not only does it not produce oxides, but is also soft and acts as a soft gasket.

4.8 Effects of Soldering

There are several problems directly attributed or related to soldering. One of them is the flow of flux. At the present time the role of the flux in generating

nonlinear products is not known. It is suspected that excess flux can cause deterioration of linear operation over a period of time.

The metal used in the solder after heating and being in a liquid state is left to harden, generally in an uncontrollable way. If the cooling is fast the crystal structure forms microscopic discontinuities and this contributes to nonlinearities.

On many occasions the soldering is done very carefully and initially the system performs quietly and well, but after some time it deteriorates. At least in some cases the deterioration was caused by mechanical stress at the solder joint which microscopically produces cracks and discontinuities in the metal. This can be cured by proper construction which removes the stress from the solder joint.

5. Experimental Linearized Hardware

In order to gain some insight into possible techniques for alleviating the problem of nonlinear generation in coaxial components, several test fixtures have been prepared for use with the METRRA equipment as a test bed. It is hoped that with these fixtures and the data obtained from them ideas concerning soldering techniques for reliable and long lasting connections may evolve. Also, better understanding of the effects of oxidation on copper contact may be gained as well as information on the effect of gold plating.

5.1 Test Fixtures

Test fixtures provided include several types of sleeves for joining the inner and outer conductors of coaxial cable as illustrated in Figures 12 and 13. There are copper sleeves and gold plated copper sleeves to be soldered to the cable. These will be inserted into the system and the harmonic levels measured before and after stressing the solder joint. Plated and unplated outer sleeves to be press fit onto the cable are also provided to gain some information on the nonlinearity of this type of purely mechanical joint.

We have also supplied two types of connecting sleeves which it is hoped will enable other test fixtures to be inserted into the test bed with a minimum of physical effort. These connectors are shorted sections, shown in Figures 14 and 15, and open $\frac{1}{2}$ wave sections of tubing, shown in Figure 16, to be placed over the outer coaxial conductor. Using these, it is hoped that accurate measurements can be made on the three commercial coaxial connectors, one SMA, one TNC and one N. This data will be used to check correlation between experimental measurements and theoretical predictions. Figure 17 illustrates a clamp for applying pressure at the contact points of the shorted sleeves. The test procedure included as Appendix E details the use of these fixtures.

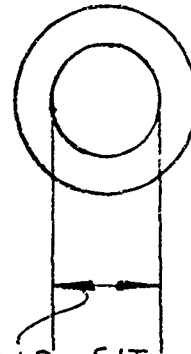
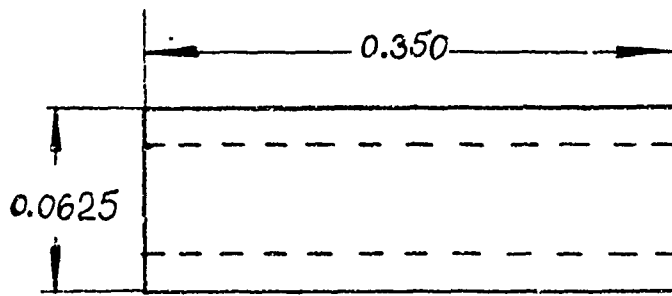
5.1.2 Filters

A comparison of the Telonic filter and the WDL filter serves to illustrate the design philosophy emphasized in this report as far as techniques for minimizing potential nonlinear sources are concerned. Figures 18 and 19 are photographs of the Telonic and Ford filters respectively. Notice the small diameter wire (.084 cm) and the solder joints between each capacitive section of the Telonic filter. Each of these joints is a potential generator and the small wire diameter compounds the problem. In the WDL filter we have tried to eliminate as many solder joints as possible by machining the filter from a single piece

of metal. In an application where low level nonlinearities are potential problems, this technique of construction is mandatory. The only solder joint of importance is the one joining the filter to the coaxial cable on the output end of the filter. Special provision has been made to relieve the stress on the solder joints at both ends of the filter. This is done by adding a short sleeve to the outer conductor of the filter into which the coaxial cable is soldered. The sleeve rather than the solder supports the cable. This should extend the length of time that the solder joint can be reliably counted upon to be acceptably linear

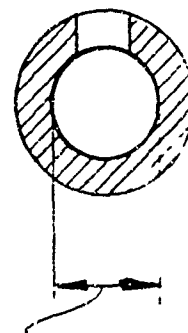
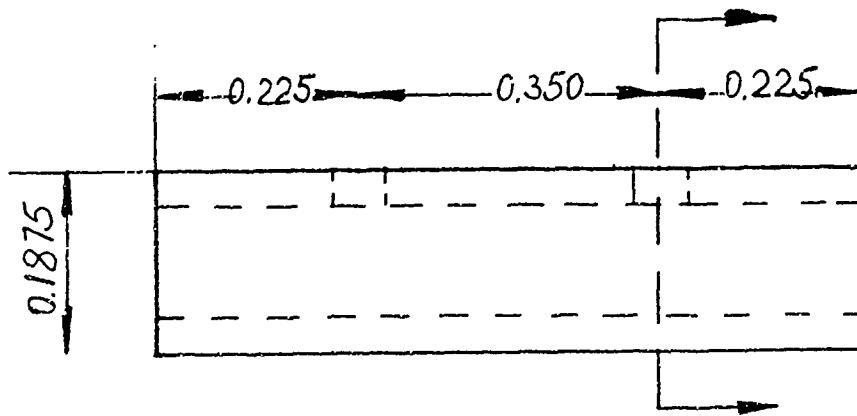
Another technique used in the Ford filter concerns the filter ends. The cylindrical outer conductor is used as a waveguide beyond cutoff to prevent leakage from the ends. This technique is so effective that the fields are attenuated at least by 40 dB even in the relatively short distance between the end of the filter's center piece and the end of the outer conductor. Now the ends may either be left open without fear of extraneous leakage or coupling, or end caps may be soldered on with confidence that the RF currents flowing in these joints will produce negligibly small levels of harmonic.

Figures 20 through 23 document the electrical characteristics of the Aeronutronic-Ford filters. It should be emphasized that this filter was made using an old design rather than generating a new filter with different electrical characteristics. This was done in order to meet time and budget constraints.



SLIP FIT OR
PRESS FIT
FOR 0.0359 ± 0.0005

FIGURE 12
COUPLER FOR THE CABLE CENTER
CONDUCTOR



SLIP FIT FOR
 0.141 ± 0.001

FIGURE 13
STANDARD SLEEVES FOR SOLDERING
ON THE CABLE JACKET

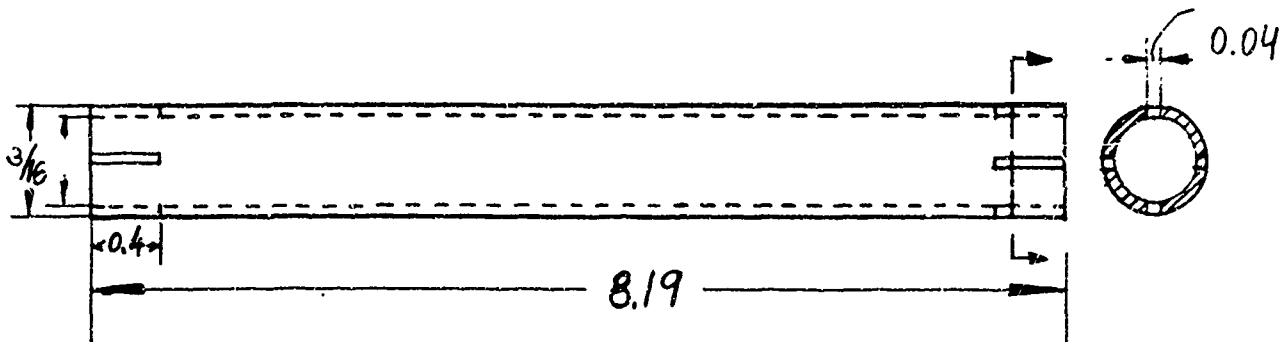


FIGURE 14
 SOLDERLESS INSULATED COUPLER SHORTED AT
 THE END BY CLAMPS 1/2 WAVELENGTH

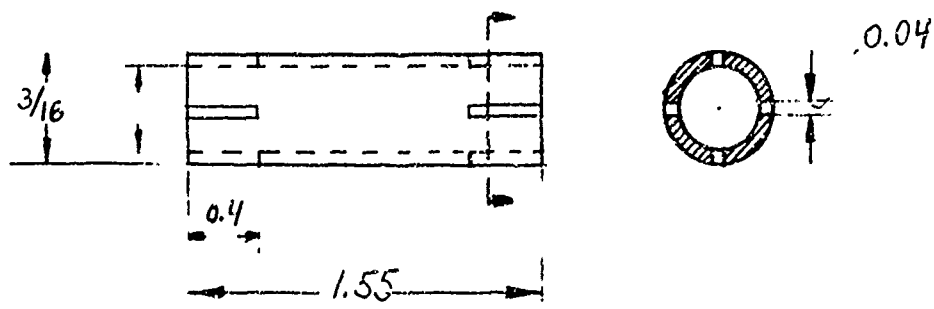


FIGURE 15
 SHORT MECHANICAL COUPLER
 SOLDERLESS NOT INSULATED

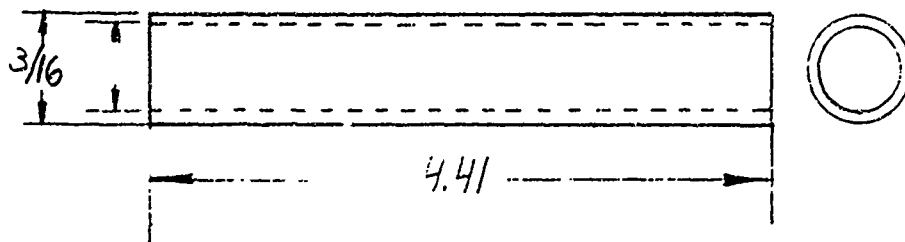


FIGURE 16
SOLDERLESS, INSULATED COUPLER
OPEN ENDED 1/4 WAVELENGTH

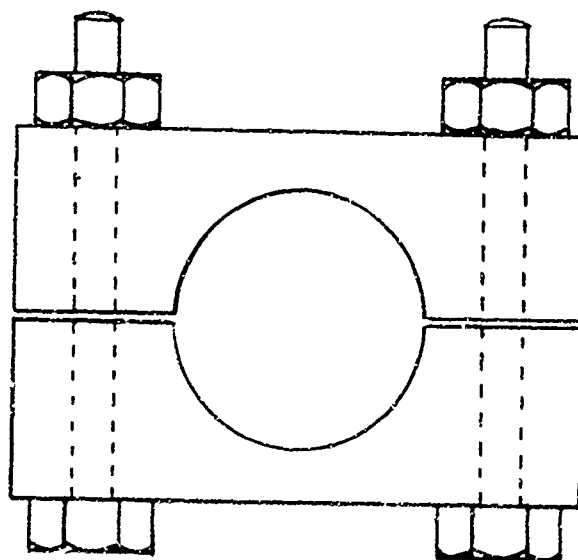


FIGURE 17
CLAMP

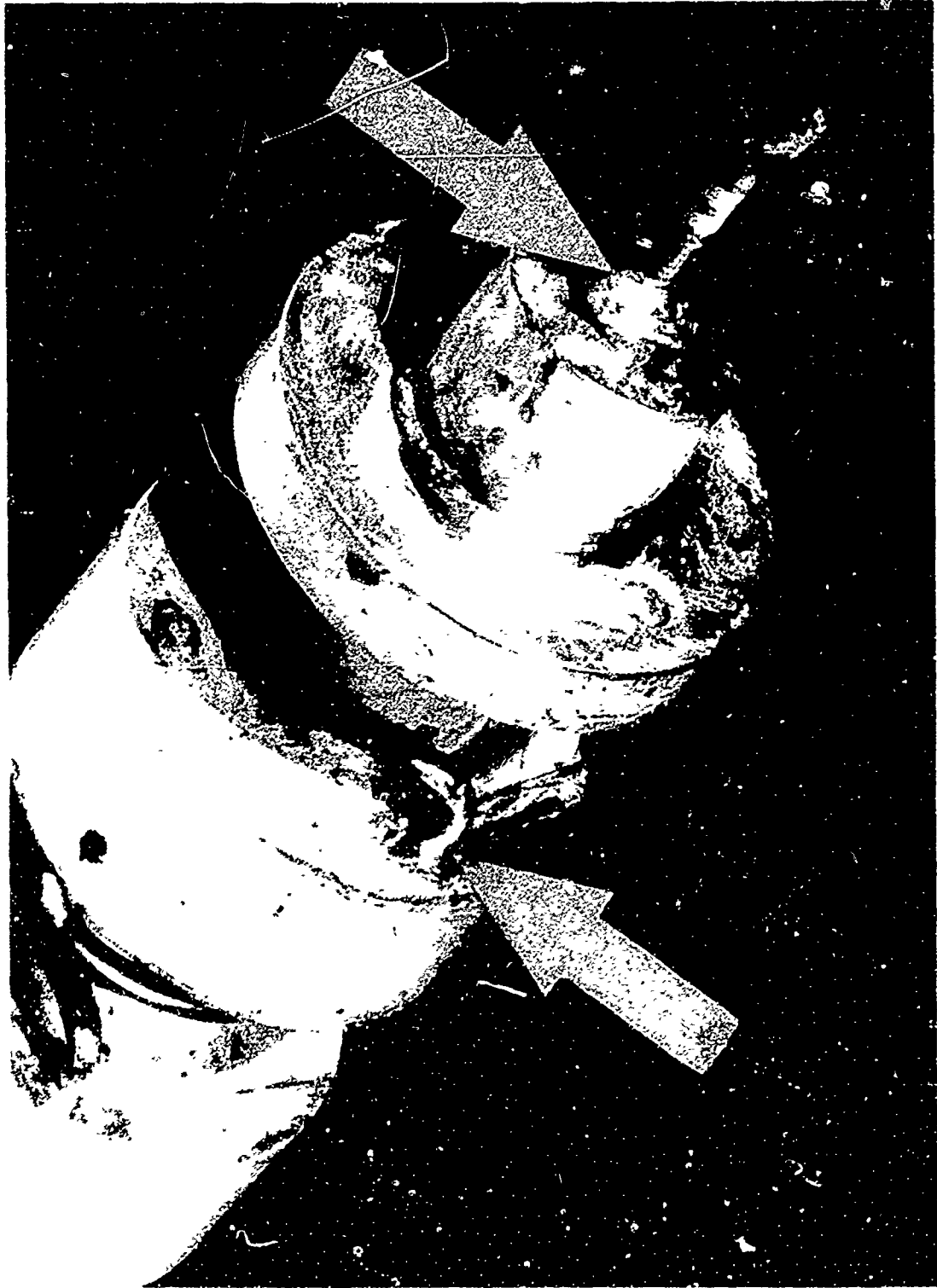


Figure 18. Internal Structure of Telonic Lowpass Filter.
Arrows Show Points of High Current Density at Metal to Metal Junctions.

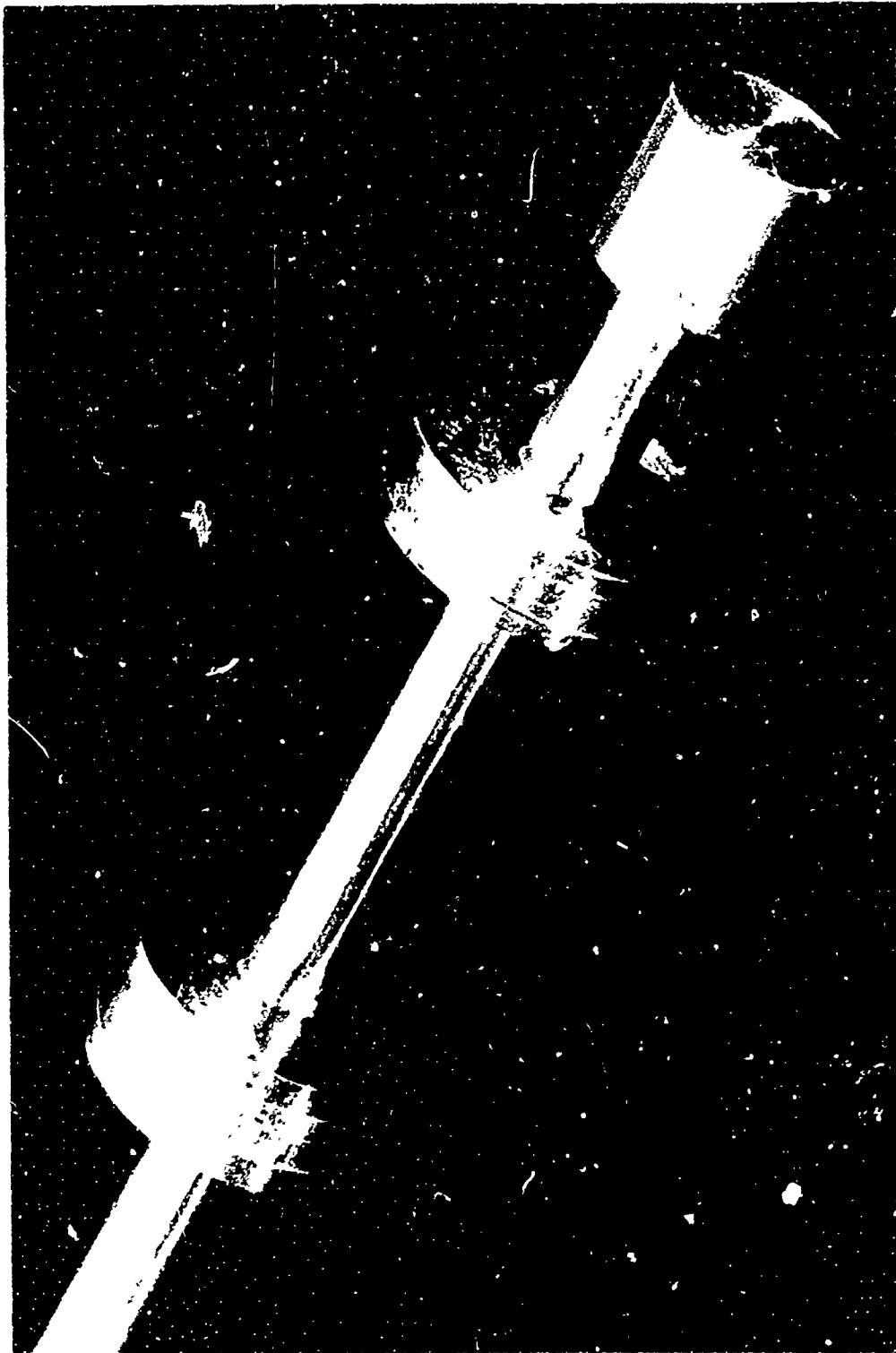
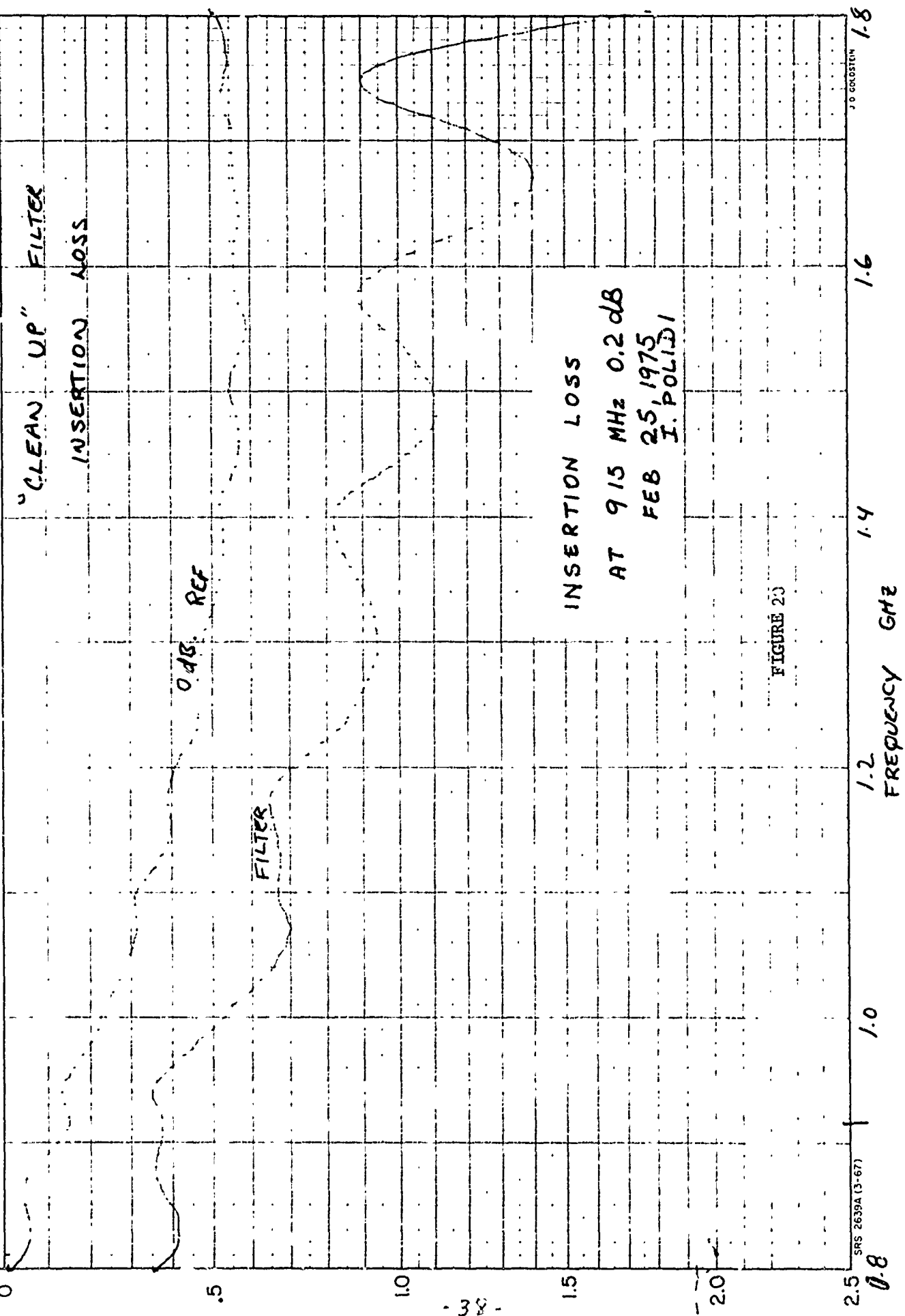


Figure 19. Internal Structure of Aeronutronics Ford Filter
Specially Constructed for Low Level Linearity



MFR _____ ID NO. _____
 MODEL _____ TEST NO. _____



INSERTION LOSS
 AT 915 MHz 0.2 dB
 FEB 25, 1975
 J. POLIDORI

FIGURE 20

J. O. GOSTEN 1-8

1.6

1.4

1.2

1.0

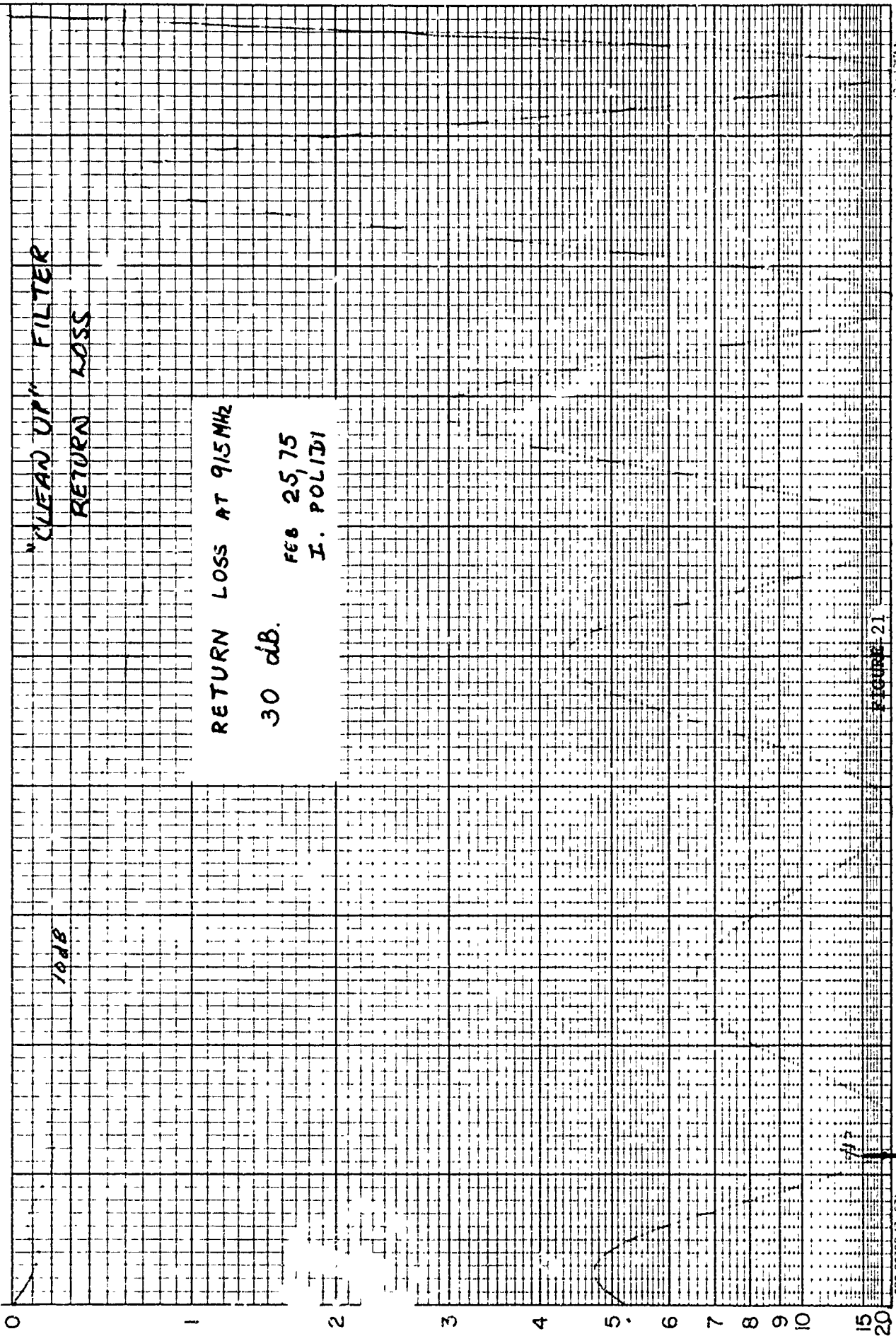
0.8

SRS 2639A (3-67)

JB



MFR _____ ID NO. _____
MODEL _____ TEST NO. _____



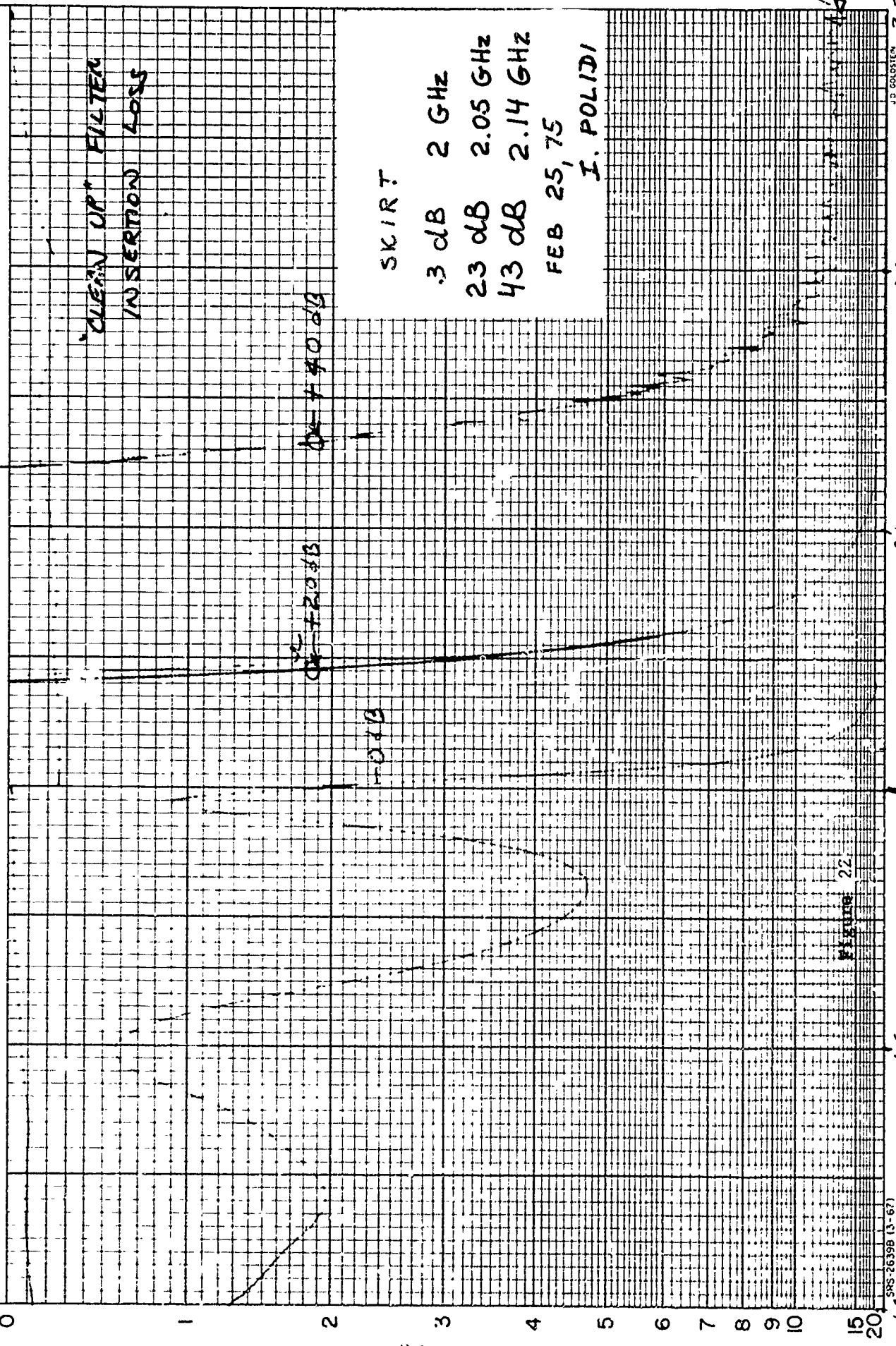
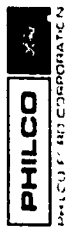
345-26398 (3-67)

FIGURE 21

JB

MFR
MODEL

ID NO.
TEST NO.



-40-

SNS-26399 (3-67)

JD GOLDSTEIN

For $F > 2.6$ GHz
Att ≈ 100 dB
I. Polidi

Low Pass "Cleanup"
Filter Characteristics

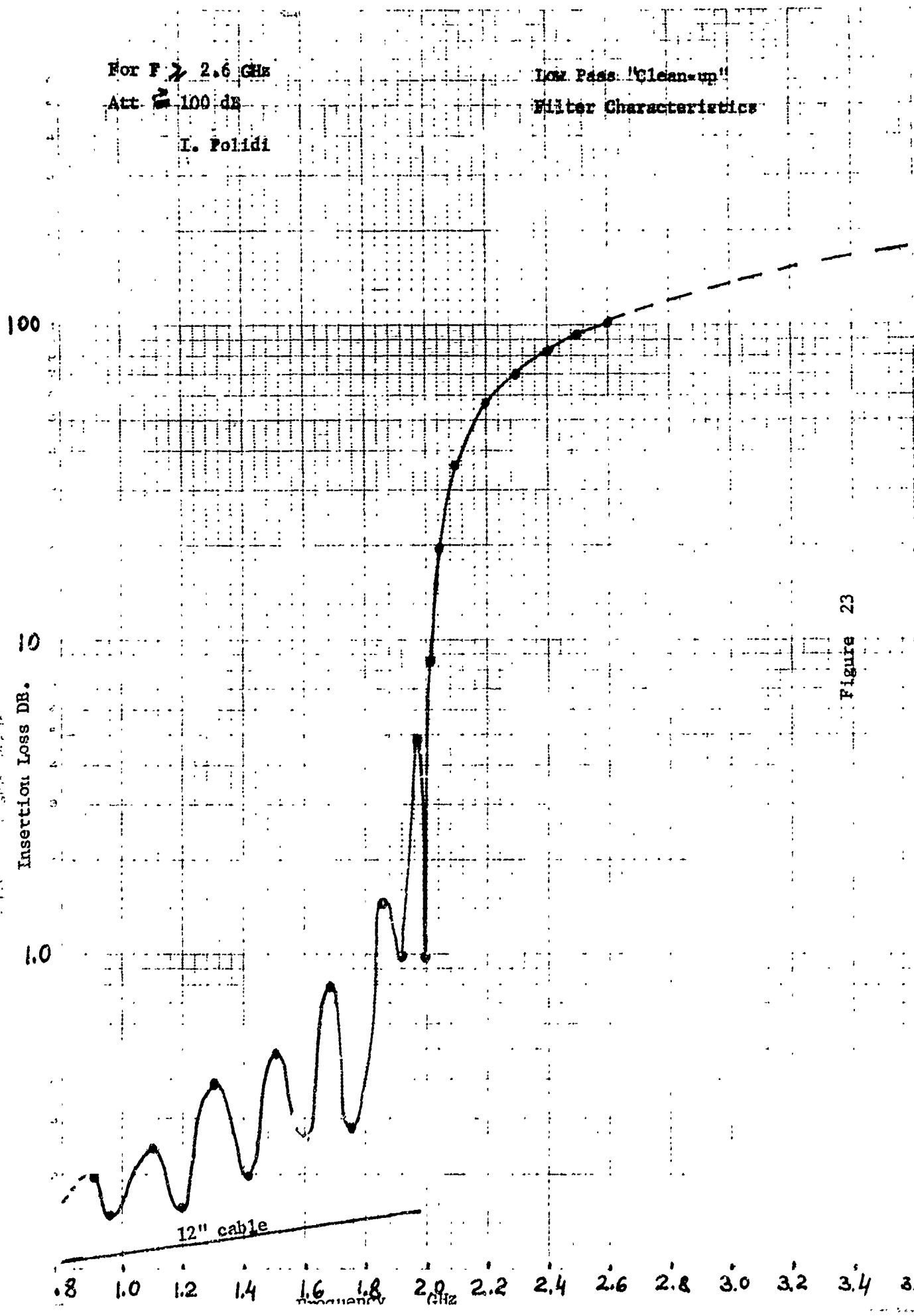


Figure 23

6. Producibility Design as Applied Directly to the METRRA Equipment

This section is a logical continuation of Section 3, where the problem areas have been identified and of Section 4, where general producibility rules have been defined. The intention here is to show how these general rules can be applied in the specific case of the METRRA problem areas and to present methods to alleviate or solve the problems. The reader will find that some of the recommendations are directed to the immediate problems and are directly and immediately applicable. Other recommendations are directed to long term goals and will require additional thoughts before incorporating them in the equipment. They are included, however, to serve as illustrations of the trend of the thoughts and will be useful in future designs.

6.1 Transmit Filter

As indicated in Section 3, the transmit filter plays a major role in the operation of the METRRA equipment and its quality will determine the quality of the combined system. The filter specification are difficult to meet. It has to conduct 2 KW of power with low insertion loss; it has to attenuate the third harmonic by 150 dB; it should prevent radiation; and it has to be lightweight in order to suit the needs of a portable instrument. In addition, the filter must be linear, i.e. it should not produce nonlinear products of its own. The standard off-the-shelf commercial units meet all the requirements except for linearity and this will be the only aspect discussed here.

As the signal propagates along the filter the third harmonic produced by the power amplifier gets attenuated and at the same time third harmonic generated in the nonlinear joints of the filter begin to appear. The newly regenerated third harmonic will be rejected by the sections of the filter located after the source. If, however, the source is in the last filter section or in the filter output there will be no obstacle in the way of the third harmonic's propagation to the antenna. It is evident that to comply with the requirement of linearity, care must be taken only at the output of the filter. Therefore, it is our recommendation to provide the filter input with a cable and connector which will allow it to be connected to the power amplifier assembly and to modify the last few sections and output of the filter.

The photo in Figure 18 shows the TELONIC low pass filter used in the transmitter

output of the METRRA validation model. In order to comply with the requirements of size and weight the inductance of the central part is realized by wire of 0.089 centimeters diameter, where the current density is 22.6 A/cm and in the joints shown by the arrows large levels of third harmonic are generated. In the next photo, Figure 19, is shown the Aeronutronics-Ford filter designed with special care to be linear. This filter is considerably larger in size; the high impedance part of the inner conductor has a diameter of .457 cm., much larger than the 0.89 cm of the TELONIC unit. The central structure of the filter is one solid piece with no junctions of any kind except for input and output. The outside conductor, carrying the same current was made several centimeters longer than the inner conductor. This attenuates the fields to such an extent that if a cap is mounted at the end of the filter there will be no generation of non-linear products. One weak point of this filter is in the output. The large filter had to be terminated to the tiny semi-rigid .141 inch cable. This defeats all the care taken with the filter. A quick computation indicates that if this cable will be replaced by 0.25 inch the improvement in reducing the harmonic generation will be 19 dB.

The central conductor of the cable was soldered to the filter and it was feared the wiggling of the cable would produce cracks in the solder. To avoid this possibility, the cable jacket was soldered to the filter outer conductor with a sleeve thereby removing the stress from the solder junction. Figure 24 illustrates the stress-removing technique.

One other weak point of this filter is its large size and weight. The size can be considerably reduced without appreciable deterioration, and the weight can be reduced by replacing the brass with aluminum. These steps can be undertaken in future designs.

An alternate idea can be implemented in the following way. One filter (the TELONIC or similar) will be used to filter the third harmonic of the transmitter. This will have small size and weight but it will produce some third harmonic of its own. If this level is precisely known, then a second filter of the type of Aeronutronic-Ford but with far fewer sections can be used to "clean up" the nonlinear products of the first filter. This version will have advantages only if the second filter has to have moderate rejection since fewer sections will then be sufficient. The exact determination of all the quantities will require

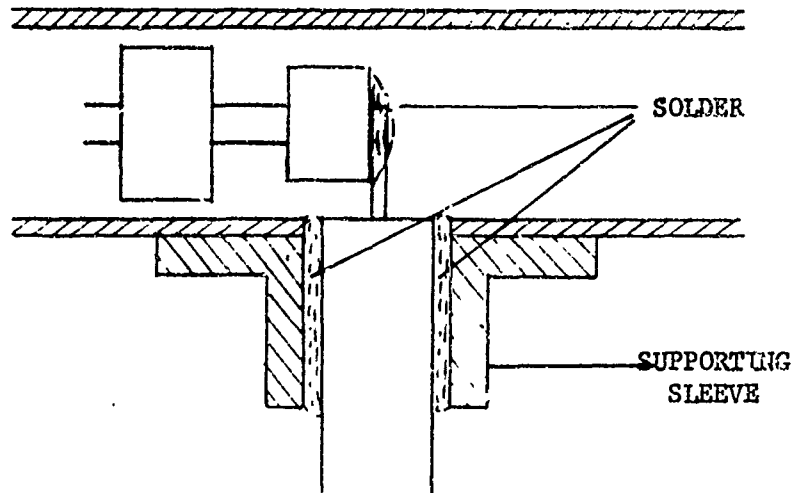


FIGURE 24
CONNECTION OF THE CABLE TO THE
FILTER OUTER CONDUCTOR. THE SUPPORTING
SLEEVE REMOVES THE STRESS FROM THE SOLDERING



Figure 25. Balun

measurements and computations and therefore can be done only as a future design.

6.2 Balun in the Transmitting Antenna

A photograph of the balun is shown in Figure 25. The balun is required to produce a balanced line from an unbalanced one and is also required to transform the 50 ohm transmission line to the 73 ohms input impedance of the dipole antenna. To these requirements must be added the requirements of linearity and even harmonic suppression. The balun has a bracket fixture used as an input; this fixture houses the .141 cable and provides the transition to microstrip line. The cable should be replaced by a larger size for the same reasons presented in Section 6.1. But even after that, the input junction will still be a source of nonlinear generation and the level of this recreated third harmonic must be established. It was planned before the last contract modification to suggest a test in which two baluns connected back to back will be inserted into the system as one test fixture and in this way measure the nonlinear generation in the balun. If this quantity is established and its magnitude is objectionable, it is our recommendation to increase the size of the balun to incorporate a band reject filter centered at the third harmonic. This filter will have the shape either as in Figure 26 or as in Figure 27.

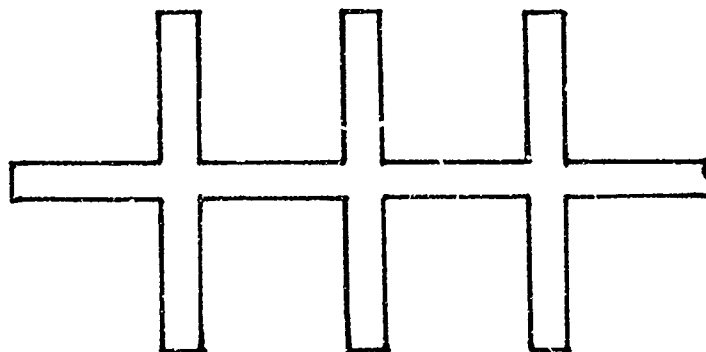


Figure 26

Band Reject Filter - Combined with the Balun

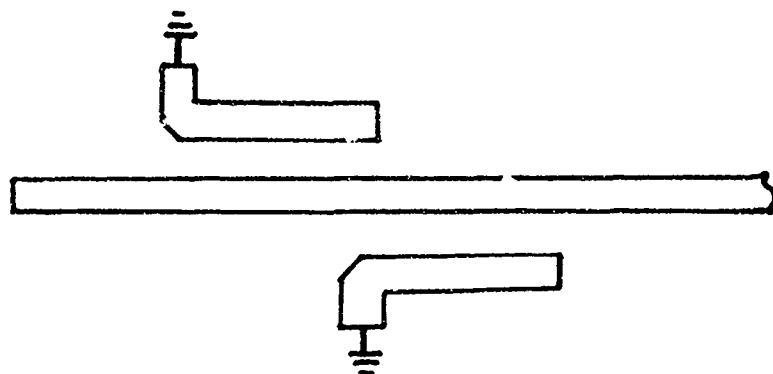


Figure 27

Band Reject Filter - Combined with the Balun (Alternate Solution)

The problem of the output terminals of the balun, where nonlinear generation also can take place remains unsolved and no easy way has been found to reduce the harmonic level at this point. Of course no step involving these additions is recommended before tests can be made establishing the need for these modifications.

6.3 Antenna Coupling

Usually a radiating, tuned narrow band antenna provides a mismatch for any other frequency and in a way acts as a "filter" passing only the proper frequencies. This is not the case in the METRRA unit since transmitted and received frequencies are harmonically related. Any third harmonic existing in the transmit antenna is efficiently radiated, picked up by the receiving antenna and arrives at the receiver. This is an unwanted signal which only confuses the operator. Every effort must be made to try to prevent the generation of third harmonic in the output of the transmitter, but since it is not possible to totally eliminate the third harmonic generation, the antennas should have high isolation at that frequency. A specification of this quantity is most appropriate. No less important is the antenna isolation at the transmit frequency. The reason for this is that if considerable power at the fundamental frequency arrives at the

receiver filter there may be spots acting as nonlinear generators and this will also desensitize the receiver. A good system design must try to establish the antenna isolation at both fundamental and third harmonic frequencies and relate these quantities to the level of the harmonic present in the transmit antenna and the level of nonlinear generation in the receiver filter. An antenna structure which can provide good isolation at both frequencies is desirable.

6.4 Receiver Filter

The receiver filter has to protect the receiver circuitry from any out of band frequency, allowing only the desired frequency to reach the receiver. It must have low loss, low weight and small size. In addition, it must be linear up to the level of the maximum power received from the transmitter. In the previous section the importance of knowing the antenna isolation at both fundamental and third harmonic was discussed. Assuming that a portion of the transmitter power has leaked into the receiver and assuming that this portion is excessive, let us see what alternatives are available: (a) Waveguide Filter - A waveguide filter can be designed to pass freely the third harmonic and to stop the fundamental transmit frequency. This idea will be a good one only if the input of the filter is linear and will not produce third harmonic because if it is generated, the filter will pass it on to the receiver. In our case, the input of the filter will be a capacitive probe not making ohmic contact and therefore free of nonlinearities. Electrically this solution is very attractive but has the disadvantage of being large and heavy.

(b) Combination of Two Filters - A number of combinations of two filters one after the other are possible either packaged together or separately. One possible combination is a high pass followed by bandpass filters. Another possibility is that the first filter will have only a minimum amount of sections but will have relatively large size. The first unit will be linear and will reject the transmitter to the extent that the remaining transmit power will not be able to produce harmonics at the second filter, which then can be designed without consideration for its linearity.

Once again it is proper to remember that it pays to go to more elaborate solutions only if the need for them is first established, which can be done either by tests or by system design and computations.

6.5 Backpack Version

The validation model of the METRRA unit was designed to be held in front of the person operating it. Recently some indications exist that it may be more advantageous to carry the unit on the back of the operator and if this is done, the antennas will have to be mounted at a height above the operator's head. This possibility offers an attractive solution to the problems since relatively large filters can be part of the structure which positions the antennas over the head of the man. In essence, the filters will no longer be part of the transceiver and that package actually can be slightly smaller.

6.6 Combined Transmit Front End

An interesting solution can be obtained by combining many considerations together. This solution is quite different and can be advised as a future redesign goal.

The input impedance of the dipole antenna is 73 ohms. If this (or 75 ohms) impedance is accepted at the transmitter output, the current will be reduced in inverse proportion to the impedance ratio. As a result, the coupling out of transmitter cavity will change, the cables will be 75 ohms, the transmit filter will be slightly different and the balun will not have the impedance transformation. None of these changes are difficult. For other reasons the filter already must be a special order; it should not be any problem to design it for 75 ohms. Next, it is planned to eliminate the cable at the filter output. The filter will terminate directly into the balun via the same type of bracket used in the balun input but with a much larger center conductor. This solution can be built in a size and weight complying with the requirements of portable equipment. It is expected that by using these ideas it will be possible to achieve very good linearity, surpassing all other version.

6.7 Chassis Considerations

Under certain conditions the metal structure used to house the electronic equipment may conduct RF currents and if these currents flow through bolt joints or solder joints there will be nonlinear product generation which easily can provide a parasitic path for leakage and can cause blocking of the receiver. To cure similar problems, it is recommended to filter properly and to direct the ground currents through separate wire, to a "single point ground," a very good practice. Bolts and rivets must be avoided; welding practices are recommended

instead. To verify the absence of this parasitic leakage the transmitter and receiver must be terminated by dummy loads. Under these conditions the received signal must be below the detectable level.

7. Program Summary, Conclusions and Recommendations

Although the majority of the work conducted in the foregoing investigation was largely analytical, a number of significant producibility concepts relative to the METRRA equipment were reached.

7.1 Data Translation

Aeronutronic-Ford has a large amount of information and data at X-Band frequencies based on past detailed theoretical and experimental work. Stable test facilities with the ability to test to IM levels of 210 dB below the carrier have been built. However, most of the previous analytical investigation, experimental data, and designs have been performed at X-Band frequencies for waveguide components and for third order intermodulation products. Therefore, in order to take advantage of this valuable base of information, it was necessary to translate the results to the METRRA system parameters of frequency and nonlinear product. For this, calculations of the effect on distortion levels when frequency is changed, effects of the variation of conductor size, effects of power variation and the relationship between third order intermodulation products and third harmonic generation were made. Out of this came the following conclusions:

- The effect of frequency change can be assumed negligible since the differences due to frequency were calculated to be small and will be masked by larger differences due to contact microgeometric differences. Therefore the X-Band results can be directly applied to the METRRA frequency.
- The generating level varies directly with current density and therefore a procedure to make predictions based on normalized current densities was developed and used.
- For purposes of estimating METRRA levels a rule of thumb based on the data from previous programs was used. That is a 2.5 dB increase in distortion for each dB increase in input power level.
- The difference between third order intermodulation and third harmonic generation is within 1.2 dB and therefore can be considered negligible.

7.2 Source Identification

Analysis of sources of nonlinear generation in the METRRA unit was performed and specific critical generating areas were identified to be in the transmitter output filter, balun and antenna and to a lesser extent, in the receiver input filter, balun and antenna.

Careful analysis of the sources lead to the conclusion that a linearized METRRA validation model could be implemented using proper design techniques to meet the specified system noise levels.

7.3 Brassboard Model Linearization

Specific attention was directed to producibility design and analysis relative to implementation of a linearized laboratory system. For this a series of general design guidelines was made (see Section 4.1). Detailed design methods were then presented and a series of specific recommendations were made for the following METRRA components:

7.3.1 Transmit Filter

A single piece design is recommended for this component thereby eliminating all metal-to-metal contacts except at the input and output. Also the geometry should be as large as practical.

7.3.2 Receiver Filter

The receiver input filter should be a nonresonant type such as a high pass filter or, a combination of an oversized prefilter to decrease the transmit signal followed by a standard small bandpass or highpass filter.

7.3.3 Antenna Isolation

Isolation between the transmitting and receiving antennas must be good, preferably around 30 dB.

7.4 Ruggedized Field Unit

For implementation of an eventual field ruggedized linear system further precautions need to be followed. The most important of these are the ideas of combining several components into one and using clean-up filtering. These concepts for ruggedized design can then be employed to remove harmonics generated due to field deterioration of system components.

For eventual implementation of a ruggedized field unit it was felt important to obtain experimental design data for linear component producibility. For this purpose a series of test fixtures were devised but at this time no data is available.

7.5 Backpack Version

A backpack METRRA unit should be easier to implement from a producibility standpoint. It is expected that the antenna will have better performance in terms of gain and isolation. The filters can be part of the pack structure so can be physically larger, thereby lowering current densities and the resultant internal harmonic generation.

The foregoing conclusions were reached based on analysis and extrapolation of X-Band test results. Although the recommendations are felt strongly to be very meaningful guidelines for producibility, much more meaningful results could be reached if future analysis is coupled with system experimentation. Therefore, it is strongly recommended that producibility test fixture experimentation be conducted in the future if possible.

Appendix A

Relation Between Third Order Intermodulation Products and Third Harmonic Generated by the Same Device

Experimental data available at Aeronutronics concerns third order intermodulation products between carriers at two different frequencies. In order to use this data for predicting third harmonic generation, a relationship between carrier power, third order intermodulation and third harmonic generation must be established.

The output response y of a non-linear device when driven by an input x may be represented as a polynomial in x

$$y = a_0 + a_1 x + a_2 x^2 + a_3 x^3 + \dots$$

where powers of x beyond the third are ignored since they contribute very little to the third order outputs. If an input x consisting of two frequencies α and β is used to excite the device we have:

$$x = A \cos \alpha + B \cos \beta$$

$$y = a_0 + a_1 (A \cos \alpha + B \cos \beta) + a_2 (A \cos \alpha + B \cos \beta)^2 + a_3 (A \cos \alpha + B \cos \beta)^3 + \dots$$

or

$$y = a_0 + a_1 (A \cos \alpha + B \cos \beta) + a_2 (A^2 \cos^2 \alpha + 2AB \cos \alpha \cos \beta + B^2 \cos^2 \beta) + a_3 (A^3 \cos^3 \alpha + A^2 B \cos^2 \alpha \cos \beta + 3AB^2 \cos \alpha \cos^2 \beta + B^3 \cos^3 \beta) \quad (1)$$

The following trigonometric identities are used to simplify (1):

$$\cos^2 \alpha = \frac{1 + \cos 2\alpha}{2}$$

$$\cos \alpha \cos \beta = 1/2 [\cos (\alpha + \beta) + \cos (\alpha - \beta)]$$

$$\cos^3 \alpha = 3/4 \cos \alpha + 1/4 \cos 3\alpha$$

Then:

$$y = a_0 + a_1 (A \cos \alpha + B \cos \beta) + a_2 \left\{ \frac{A^2}{2} (1 + \cos 2\alpha) + AB [(\cos \alpha \cos \beta) + \cos (\alpha - \beta)] + \frac{B^2}{2} (1 + \cos 2\beta) \right\}$$

$$+a_3 \left[\frac{3A^2}{4} \cos \alpha + \frac{A^3}{4} \cos 3\alpha + \frac{3}{2} A^2 B (1 + \cos 2\alpha) \cos \beta + \frac{3}{2} A^2 B \cos \alpha (1 + \cos 2\beta) + \frac{3B^3}{4} \cos \beta + \frac{B^3}{4} \cos 3\beta \right]$$

The term in brackets following a_3 simplifies further to $\frac{3A^2}{4} \cos \alpha + \frac{3A^3}{4} \cos 3\alpha + \frac{3}{2} A^2 B [\cos(\alpha + \beta) + \cos(\alpha - \beta)] + \frac{3}{2} AB^2 [\cos(\alpha + 2\beta) + \cos(\alpha - 2\beta)] + \frac{3}{4} A^2 B \cos \beta + \frac{3}{4} B^3 \cos 3\beta$

Now, grouping the terms appropriately we obtain:

$y = a_0 + \frac{a_2 A^2}{2} + \frac{a_2 B^2}{2}$	DC Term
$+ (a_1 A + \frac{3a_3 A^3}{4} + \frac{3a_3}{2} A^2 B) \cos \alpha$	Fundamental in α
$+ (a_1 B + \frac{3a_3 B^3}{4} + \frac{3a_3}{2} A^2 B) \cos \beta$	Fundamental in β
$+ \frac{a_2 A^2}{2} \cos 2\alpha$	2nd Harmonic in α
$+ \frac{a_2 B^2}{2} \cos 2\beta$	2nd Harmonic in β
$+ \frac{a_3}{4} A^3 \cos 3\alpha$	3rd Harmonic in α
$+ \frac{a_3}{4} B^3 \cos 3\beta$	3rd Harmonic in β
$+ \frac{a_2 AB}{2} [\cos(\alpha - \beta) + \cos(\alpha + \beta)]$	2nd Order Products
$+ \frac{3a_3 A^2 B}{4} [\cos(2\alpha + \beta) + \cos(2\alpha - \beta)]$	3rd Order Products
$+ \frac{3a_3 AB^2}{4} [\cos(\alpha + 2\beta) + \cos(\alpha - 2\beta)]$	

For the two carrier case:

$$P_T = P_A + P_B$$

where P_T = total input power

P_A = power in carrier A

P_B = power in carrier B

The Aeronutronic data is for the case where $P_A = 3P_B$ and for the IM r...

$2\alpha - \beta$

$$P_A = \frac{3}{4} P_T$$

$$P_B = \frac{1}{4} P_T$$

$$A = \sqrt{2P_A Z} = \sqrt{\frac{3}{2} P_T Z}$$

$$B = \sqrt{\frac{1}{2} P_T Z}$$

The coefficient for $\cos(2\omega - \beta)$ becomes $\frac{3a_3}{4} (\frac{3}{2} P_T Z) (\frac{1}{2} P_T Z)^{\frac{1}{2}} = \frac{a_3}{8} \frac{(P_T Z)^{\frac{3}{2}}}{2^{\frac{1}{2}}}$

For the single carrier case let P_T be the same as in the two carrier case and

let $B = 0$ then $A = \sqrt{2P_T Z}$ and the coefficient for the third harmonic is:

$$\frac{a_3}{4} (2P_T Z)^{\frac{3}{2}}$$

Taking the ratio of the third harmonic coefficient to the third order coefficient:

$$\frac{\frac{a_3}{4} (2P_T Z)^{\frac{3}{2}}}{\frac{9}{8} a_3 \frac{(P_T Z)^{\frac{3}{2}}}{\sqrt{2}}} = \frac{8}{9} = .89$$

taking the ratio in dB

$$\frac{\text{3rd Harmonic}}{\text{3rd Order}} = 20 \log .89 = -1.02\text{dB}$$

which is less than the accuracy of the measurements available. Therefore, the data generated for third order products will be assumed to apply to third harmonic levels without corrections.

Appendix B

Frequency Translation of Experimental Data

Intermodulation products have been observed in waveguide at X-Band. It is necessary to use this data for making predictions for the project being reported on. It is necessary to consider the effects a change of frequency from X-Band to S-Band will have on the predictions.

We have seen the equivalent circuit of an A spot to be as shown in Figure B-1 where the non-linear junction is shown being driven by a generator of impedance R_g and feeding a load R_L . The transfer function of the network is:

$$\frac{V_o}{V_{IN}} = \frac{1 + j\omega RC}{1 + \frac{R}{R_g + R_L} + j\omega RC}$$

The Bode plot for this function is shown in Figure B-2 where it is assumed that $\frac{R}{R_g + R_L} \gg 1$. If this condition is not met, then the minimum and maximum attenuation levels approach each other while the two break frequencies also move together until the corners in the Bode plot cease to exist.

The values in the above equations are unknown. However, the attenuation observed has never been considerable, in fact it is below the accuracy of the measurements. This indicates that the two corner frequencies probably do not exist and the attenuation remains very low for all frequencies. Consequently, the level of non-linear products does not vary significantly with frequency.

Another possible mechanism for non-linear generation is microscopic discharge between two "rough" surfaces. This can occur if the two surfaces are forming imperfect contact. A. D. McDonald, in his book Microwave Breakdown in Gases (Wiley, 1966), has shown the effects of gas mixture, pressure and frequency on the breakdown of gases subjected to a microwave field. From his Figure 1-6, we

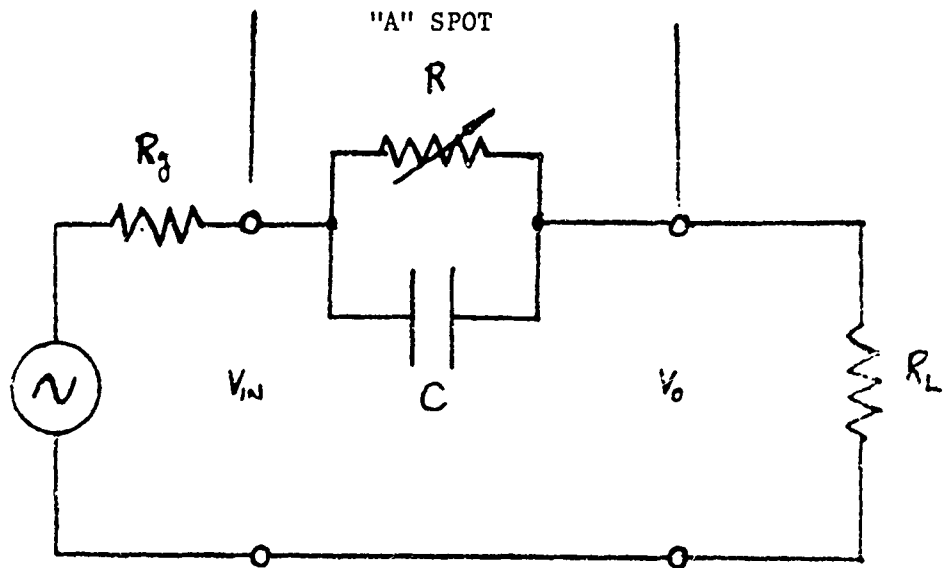


Figure B-1

Equivalent Circuit of an "A" Spot Being Driven by a Generator

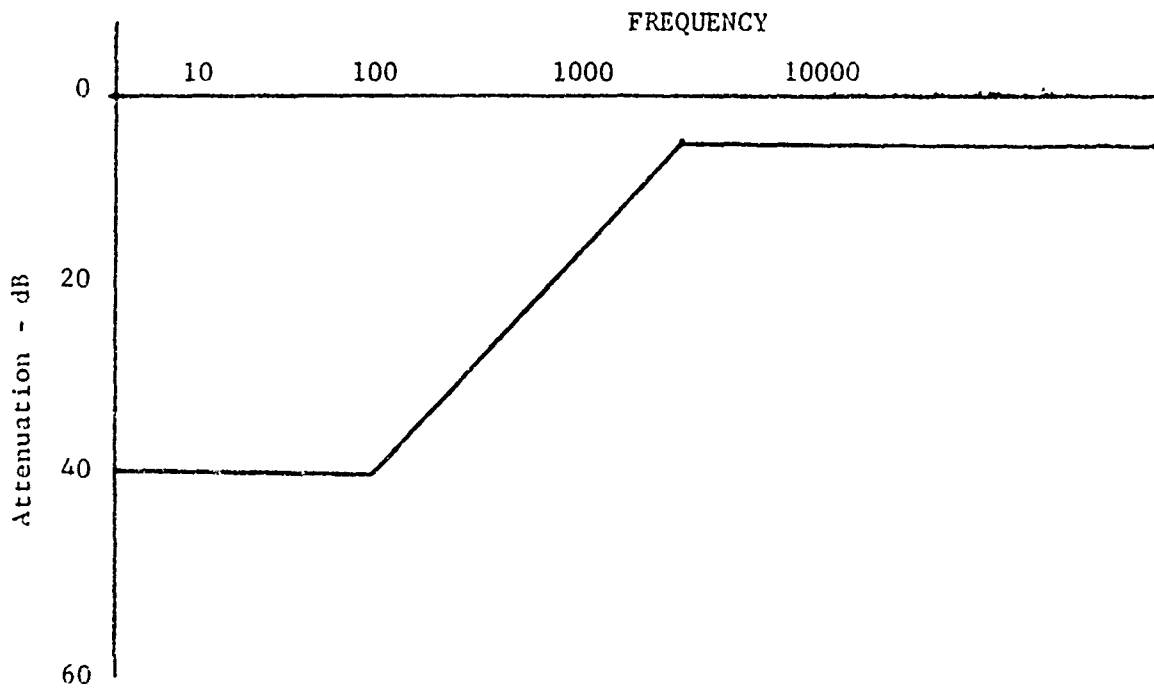


Figure B-2

Frequency Response of the Transfer Function of the Network of Figure B-1

can conclude that at atmospheric pressure, the tendency of a gas to breakdown is essentially independent of frequency.

The conclusion then, at least for tunneling, semiconductor junction and microdischarge is that no frequency effects should be observed. Since these three mechanisms are believed to be major contributors to the non-linearities, we will use the data taken at X-Band for predictions at S-Band without corrections for frequency change.

Appendix C

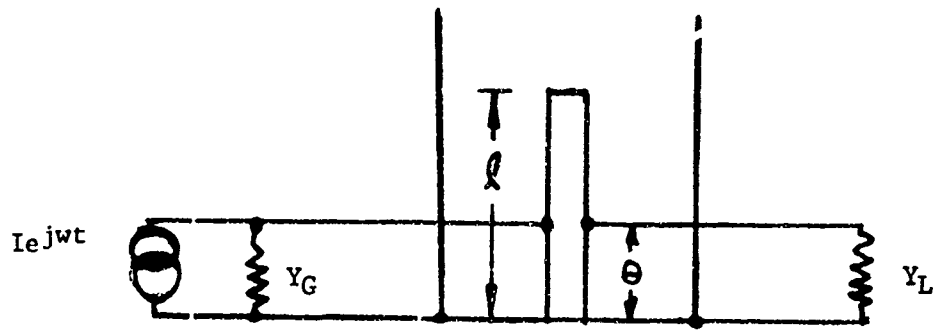
Calculation of the Currents in a Resonant Cavity at a Frequency Far from Resonance

How important is the linearity of the METRRA receiver bandpass filter when the equipment is used as a test bed and the filter is being hit with approximately 200 watts of power? The following analysis will show what happens in the case of a parallel resonant type filter structure and should indicate why this type of filter can be a critical component in the linearity of the system.

This derivation is general even though it was carried out for the specific case of a $\frac{1}{2}$ wavelength coaxial cavity. The results obtained in this derivation apply to any parallel resonant structure. In other words, the current at the shorted end of the resonator as calculated here should be the same as present in the inductive arm (below resonance) of a lumped parallel resonant circuit of the same loaded Q as the cavity.

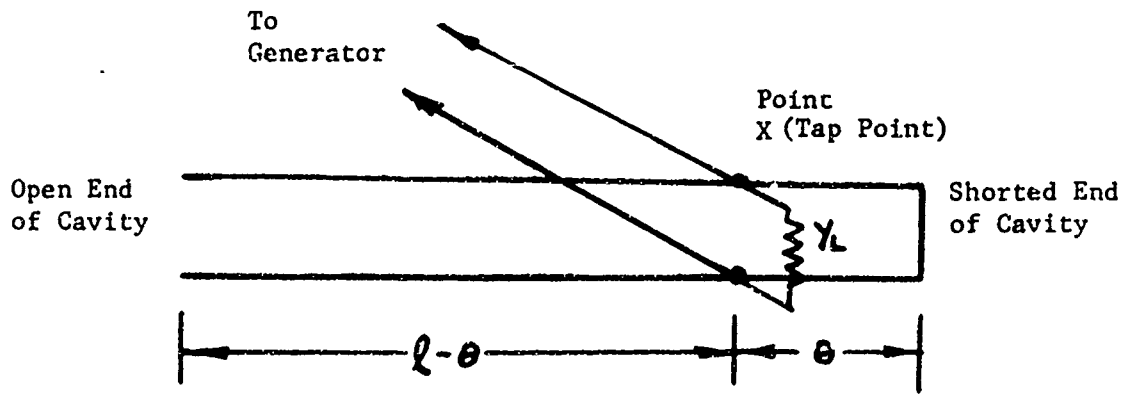
The cavity consists of a coaxial line, shorted at one end, with a load across it somewhere away from the shorted end. The generator and load are assumed matched at resonance and, furthermore, to be of equal impedance. This makes the tap point of the load the same as the tap point for the generator. No generality is lost here because for a matched load the generator sees a 50 ohm load at its tap point no matter what the true load resistance is. Figure C1 is a diagram of the circuit. Figure 2 illustrates how the cavity can be considered to be made up of two lengths of transmission lines in parallel, one shorted at the end, the other open. This will be the basis for the following analysis.

The admittance and reflection coefficient at point x , the tap point, are calculated from the transmission line equations:



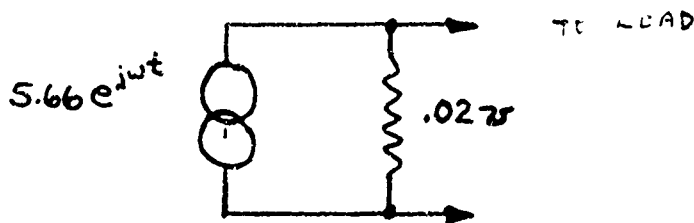
Cavity and Generator

Figure C - 1



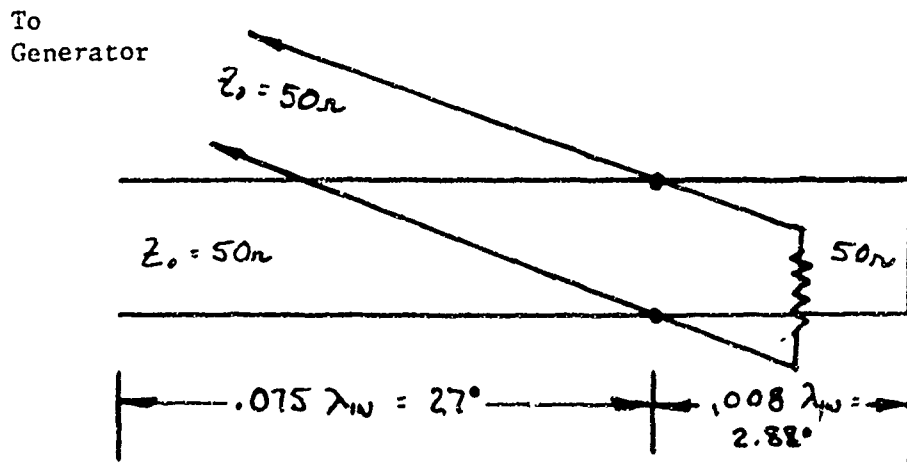
Transmission Line Equivalent to the Resonant Cavity

Figure C - 2



Generator Capable of Delivering 200 Watts to a 50 Load

Figure C - 3



Equivalent Cavity Circuit Used in the Example

Figure C - 4

From equation (1):

$$Y_x = 20 - j397.55 + j 10.19 = 387 \angle -82.04^\circ \text{ millimhos}$$

From (2):

$$P_x = \frac{.02 \cdot 387 \angle -82.04^\circ}{.02 + 387 \angle -82.04^\circ} = .99 \angle 174.10^\circ$$

Then from (3):

$$I_x = \frac{5.66}{2} - (.99 \angle 174.10^\circ) \left(\frac{5.66}{2} \right) \\ = 5.64 \angle -2.94^\circ \text{ amperes}$$

and from (5):

$$I_{\text{short } x} = 5.64 \angle -2.94^\circ \frac{-j20 \left(\cot \frac{2\pi \cdot 0.008}{\lambda} \right)}{387x \angle -82.04^\circ} \\ = 5.63 \angle -5.90^\circ \text{ amperes}$$

Then the current at the actual short is:

$$I_{\text{short}} = \frac{5.63}{\cos \frac{2\pi (.008)}{\lambda}} = 5.64 \text{ amperes}$$

This result indicates that almost the entire generator current is flowing in the first section of the filter at the short.

from the equivalent circuit:

$$Y_x = Y_L + j Y_0 \tan \frac{2\pi (l - \theta)}{\lambda} - j Y_0 \cot \frac{2\pi \theta}{\lambda} \quad (1)$$

$$\rho_x = \frac{Y_0 - Y_x}{Y_0 + Y_x} = \frac{Y_0 - Y_L - j \left\{ Y_0 \left[\tan \frac{2\pi (l - \theta)}{\lambda} - \cot \frac{2\pi \theta}{\lambda} \right] \right\}}{Y_0 + Y_L + j \left\{ Y_0 \left[\tan \frac{2\pi (l - \theta)}{\lambda} - \cot \frac{2\pi \theta}{\lambda} \right] \right\}} \quad (2)$$

The current in the forward wave from the generator is just the current which would be delivered to a matched load, or $\text{Re } \frac{I}{2} e^{j\omega t}$ in this case. The total current at point x is the resultant of the forward current and the reflected current or:

$$I_x = \frac{I}{2} - \rho \frac{I}{2} \quad (3)$$

where the negative sign arises because the reflection coefficient is defined in terms of voltages and reflected current is always 180 degrees out of phase with the reflected voltage. Then:

$$I_x = \frac{I}{2} \left\{ 1 - \frac{Y_0 - Y_L - j Y_0 \left[\tan \frac{2\pi (l - \theta)}{\lambda} - \cot \frac{2\pi \theta}{\lambda} \right]}{Y_0 + Y_L - j Y_0 \left[\tan \frac{2\pi (l - \theta)}{\lambda} - \cot \frac{2\pi \theta}{\lambda} \right]} \right\} \quad (4)$$

By using the laws of current division we can calculate the current flowing at x in the shorted section of line. Let $I_{x\text{short}}$ be the resultant current in the shorted line at point x.

$$\begin{aligned} I_{\text{short } x} &= I_x \frac{Y_{\text{short } x}}{Y_x} \\ &= \frac{-j I Y_0 \cot \frac{2\pi \theta}{\lambda}}{Y_0 + Y_L + j Y_0 \left[\tan \frac{2\pi (l - \theta)}{\lambda} - \cot \frac{2\pi \theta}{\lambda} \right]} \end{aligned} \quad (5)$$

after simplification.

But the point x is $\frac{\theta}{\lambda}$ wavelengths from the actual short and since there is a pure standing wave on the shorted section, a current maximum must exist at the short, with the current following a **|cosine|** distribution from there. Therefore, the current flowing in the actual short is:

$$I_{\text{short}} = \frac{I_{\text{short } x}}{\left| \cos \frac{2\pi \theta}{\lambda} \right|} \quad (6)$$

or:

$$I_{\text{short}} = \frac{-j I Y_0}{\sin \frac{2\pi \theta}{\lambda} \left\{ Y_0 + Y_L + j Y_0 \left[\tan \frac{2\pi (L - \theta)}{\lambda} - \cot \frac{2\pi \theta}{\lambda} \right] \right\}}$$

This is the result we have been aiming for. However, it may be of interest to know the current in the load also and this is a simple step from here:

The current flowing at some point z in the transmission line feeding the cavity is:

$$I(z) = I_+(z) - \rho I_+(z)$$

where $I_+(z)$ and $I_-(z)$ represent the forward and reflected current waves respectively.

This equation can be reformulated as:

$$I(z) = \rho I_+(z) - \rho I_+(z) + (1 - \rho) I_+(z).$$

In words, the current on a transmission line can be considered to be made up of a pure standing wave superimposed on a forward traveling wave. The traveling wave portion of the current must be completely absorbed by the load, otherwise there would be another reflection to add to the standing wave. Therefore, the average power in the load must be:

$$P_L = \frac{I}{2} (1 - \rho)^2 \frac{R_L}{2} = \frac{I^2 R_L}{8} (1 - \rho)^2 \text{ watts}$$

Example:

Let the generator be capable of delivering 200 watts to a 50 ohm load. This corresponds to the case of a 2KW generator followed by a 10dB pad. Let the cavity be resonant ($\frac{1}{2}$ wave) at some frequency and let the input frequency be $\frac{1}{3}$ of the resonant frequency. If the tap point is .024 wavelengths from the short at the resonant frequency and Z_0 for the cavity is 50 ohms then the loaded Q of the cavity is:

$$Q_L = \frac{\pi R_L}{4 Z_0 \sin^2 \frac{2\pi \theta}{\lambda}} = \frac{\pi (50)}{4(50) \sin^2 [2\pi (.024)]} = 34.8$$

which is a reasonable value for the input section of a narrowband filter. The generator model is shown in figure C - 3, and the cavity is shown in Figure C - 4 where all wavelengths are referred to the input frequency

Appendix D

Computation of the Radiated Power by a Contactless Cable Coupler

The cable coupler discussed here is shown in the next Figure, D-1. The semirigid cable is cut in two and the center pin is left some small length out of the cable.

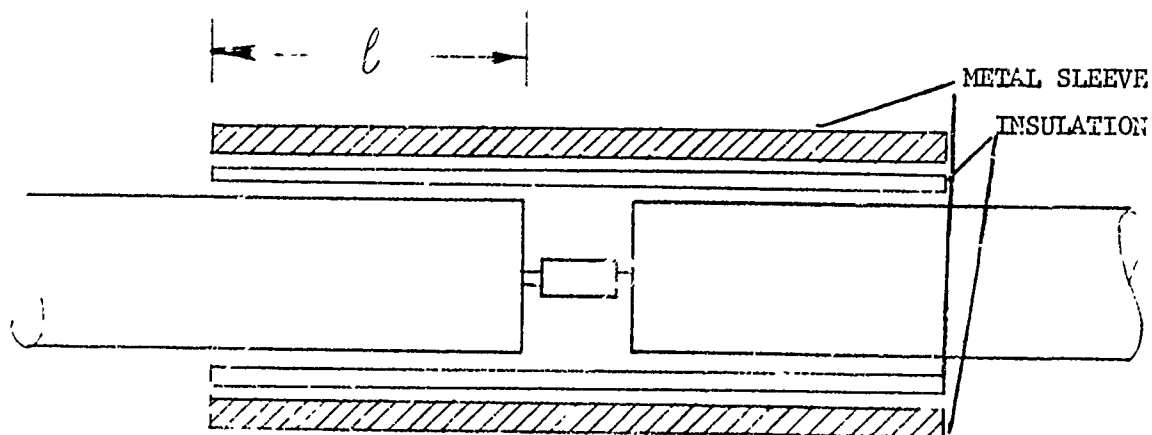


Figure D-1 - Detail of Insulated Coupler

A small coupler is used to connect the center pin either by soldering or by pressure. Since the parts are accessible there it is possible to perform high quality workmanship. The outside sleeve can be soldered too but the quality of the soldering cannot be controlled and there is a good possibility that the solder flux will flow inside the opening and become a source for nonlinear generation. In the present solution shown in the figure, the cable is wrapped with a thin insulating layer and the tubular sleeve is mounted over the insulation layer. The cable jackets, the insulator and the metal sleeve form a new coaxial line, propagating in TEM mode (i.e. propagates at all frequencies) with very low characteristic impedance Z_{0L} which is estimated to be of the order of 1 ohm. The distance, l , in the figure has been selected to be $\lambda/4$; then the open ended line will reflect zero impedance at the edge of the cable jacket, thus it will provide a low loss path for the current. However, the open end of the newly formed line can radiate energy to the free space. To be able to compute this leakage the coupler arrangement is presented in the following equivalent schematic. See Figure D-2.

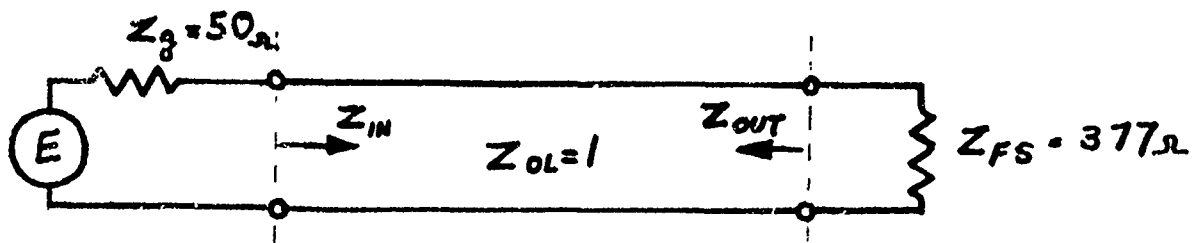


Figure D-2

The semirigid cable is presented as a generator with impedance $Z_g=50\text{ohms}$, the open ended cable has a length of $\lambda/4$, characteristic impedance of Z_{OL} , has no losses and is terminated in the impedance of free space $Z_{FS} = 377 \text{ ohms}$. At the plane 1 the input impedance can be computed using the relation:

$$Z_i = Z_o \frac{Z_L \cos \beta l + j Z_o \sin \beta l}{Z_o \cos \beta l + j Z_L \sin \beta l}$$

where:

$$Z_o = Z_{oL}$$

$$Z_L = Z_{FS}$$

$$\beta l = \frac{\pi}{2}$$

$$\cos \beta l = 0$$

$$\sin \beta l = 1$$

$$Z_i = \frac{Z_o^2}{Z_L} = \frac{Z_{oL}^2}{Z_{FS}} = \frac{1}{377}$$

At the input the reflection coefficient is:

$$\rho = \frac{Z_g - Z_i}{Z_g + Z_i} = \frac{50 - (1/377)}{50 + (1/377)} = 9998939048$$

to which corresponds the return loss:

$$RL = 20 \log_{10} \rho = -0.00092 \text{ dB}$$

but the return loss relates the ratio of reflected and incident power according to the expression:

$$RL = 10 \log_{10} \frac{P_R}{P_I}$$

and from here:

$$\frac{P_R}{P_I} = 0.99788$$

It is shown that the incident power is a nominal 2000 W, therefore the reflected power is:

$$P_R = 0.99788 \quad P_I = 0.99788 \times 2000 = 1995.76 \text{ W}$$

and finally the power forwarded through the new cable is:

$$P_F = P_I - P_R = 2000 - 1995.74 = 4.24 \text{ Watts.}$$

This power propagates without loss until it reaches plane 2 where a second reflection is produced. To compute this reflection, the cable output impedance must be computed using the same formula:

$$Z_{out} = Z_0 \frac{Z_L \cos \rho l + jZ_0 \sin \rho l}{Z_0 \cos \rho l + jZ_L \sin \rho l}$$

where:

$$Z_0 = Z_{oL}$$

$$Z_L = Z_g$$

$$\rho l = \frac{\pi}{2}$$

then:

$$Z_{out} = \frac{Z_{oL}^2}{Z_g} = \frac{1}{50} = 0.02$$

Now the reflection coefficient is:

$$\rho = \frac{Z_{FS} - Z_{out}}{Z_{FS} + Z_{out}} = \frac{377 - 0.02}{377 + 0.02} = \frac{376.98}{377.02}$$

Return loss:

$$RL = 20 \log_{10} \rho = -0.0009215$$

$$RL = 10 \log_{10} \frac{P_R}{P_I}$$

from which is found:

$$\frac{P_R}{P_I} = 0.99978$$

and since $P_I = 4.24$ Watts, the reflected power is:

$$P_R = 0.99978 \times 4.24 = 4.2386 \text{ Watts}$$

and the forwarded (radiated) power is:

$$P_F = P_I - P_R = 4.24 - 4.2386 = 0.00089954.$$

The radiated power compared with the original incident power defines the isolation:

$$I = 10 \log_{10} \frac{P_F}{P_I} = 10 \log_{10} \frac{0.00089}{2090} = \underline{\underline{-64dB}}$$

Appendix E

Test Procedure for Phase II
of the
METRRRA Producibility Engineering Investigation

Test Procedure

Purpose:

From the following tests some better insight into the problem of creating low intermodulation producing (linear) junctions in coaxial cable should be gained. The information derived from these tests will be the only available data that has been taken in a systematic manner on coaxial cables and therefore should be an extremely valuable aid for further investigation into the problems of harmonic production being experienced with this piece of equipment.

1. Measure radiated pickup level. Do this by terminating the transmitter in a high power load as shown in figure 1. Also terminate the receiver. Turn the system on and measure the third harmonic level present, if any.
2. Close the test bed system as shown in figure 2 and measure the third harmonic level at the receiver.
3. Insert the supplied filter into the system at the point shown in figure 3. Use soldered center pins and outer sleeves on the transmitter side. The receiver side will use the mechanical couplers. There are three different lengths of couplers, the largest two of which are to be used with .002 inch mylar tape as a dielectric between the outer conductor of the coax and the coupling sleeve. The longest and shortest outer sleeves are to be clamped tightly to the cable, making an electrical contact at the clamp, while the middle size sleeve should be centered over the splice and held in place with some tape. These couplers are illustrated in figures 5 through 8.

Starting with the shortest outer sleeve connect the receiver end of the filter to the system. Measure and record the third harmonic level.

Remove the mechanical coupler, prepare the cable with mylar tape and reconnect the receiver end using the non-contacting, intermediate length coupler. Measure and record the third harmonic level.

Repeat the above sequence using the longest mechanical coupler. Measure and record the third harmonic level.

If one type of the mechanical couplers showed an outstanding performance compared to the others, continue to use that type throughout the rest of the procedure. If none of the signal levels were satisfactory, try using a soldered outer sleeve on the receiver end.

In the event that the third harmonic cannot be reduced to a satisfactory level after following the above steps, it is probable that the receiver bandpass filter is causing some of the problem. To check this and reduce the effect, increase the length of cable that is being used for attenuation. If the length is increased from that which gives six decibels of attenuation to the length necessary for 10dB (about 86 ft. of .141 dia semi rigid cable), the third harmonic level should drop by 2.5 dB for each dB of decrease in power arriving at the bandpass filter, or in this case, by 10dB.

4. Insert the straight piece of coax ("dummy" test fixture) as shown in figure 4, using the mechanical couplers and soldered center pins. Measure and record the third harmonic level. If the third harmonic level using mechanical couplers represents an unacceptable value, substitute soldered sleeves and remeasure the third harmonic level and use soldered sleeves in all subsequent tests. Otherwise proceed to step 5.

5. Insert the test fixtures with the type N, TNC, and SMA connectors, one pair at a time, in place of the dummy fixture, using soldered center pins and the best outer connector system as determined in previous steps. Measure and record the third harmonic levels for each commercial connector when they are tightened to the following torques: 1, 2, 5, 10, 15, and 20 in-oz.

6. Measure and record the third harmonic level for each of the following test fixtures.

- a) Press fit center pin and soldered sleeve, unplated
- b) Press fit center pin and soldered sleeve, gold plated
- c) Soldered center pin and sleeve

7. Take two sections of coax and join them with a soldered center pin and sleeve. Insert in the test bed and measure the third harmonic level.

Now stress the connection by flexing it 10 times with a deflection of about 0.2 inches at the connection, while holding the two ends stationary. Measure and record the third harmonic level.

If the third harmonic increased by more than 3dB in the last step, reheat the outer sleeve soldered connections. Measure and record third harmonic level.

8. Take the gold plated press fit center pin from step 6 and stress it as in step 7. Solder an outer sleeve in place and measure the third harmonic level. Remove the outer sleeve, flow coat the center conductor, being careful not to get the coating on the outer conductor. Replace the outer sleeve and measure the third harmonic level, recording the results on the data sheet.

9. Remove all test fixtures from the system, and remeasure the third harmonic in the setup of figure 3. Remove the cleanup filter and flow coat the center rod as directed in separate instructions. Replace the filter and measure the third harmonic level.

Test Result Summary

- | | | |
|---|-------|-----|
| 1. Radiated pickup third harmonic level | _____ | dBm |
| 2. Beginning system third harmonic level | _____ | dBm |
| 3. Third harmonic level with Philco supplied filter and
short mechanical coupler | _____ | dBm |
| intermediate mechanical coupler | _____ | dBm |
| long mechanical coupler | _____ | dBm |
| soldered mechanical coupler (if necessary) | _____ | dBm |
| 4. Third harmonic level with dummy fixture | _____ | dBm |
| 5. Third harmonic level with SMA Connector | | |
| 1 oz-in | _____ | dBm |
| 2 oz-in | _____ | dBm |
| 5 oz-in | _____ | dBm |
| 10 oz-in | _____ | dBm |
| 15 oz-in | _____ | dBm |
| 20 oz-in | _____ | dBm |
| Type N Connector | | |
| 1 oz-in | _____ | dBm |
| 2 oz-in | _____ | dBm |
| 5 oz-in | _____ | dBm |
| 10 oz-in | _____ | dBm |
| 15 oz-in | _____ | dBm |
| 20 oz-in | _____ | dBm |
| Type TNC Connector | | |
| 1 oz-in | _____ | dBm |
| 2 oz-in | _____ | dBm |
| 5 oz-in | _____ | dBm |
| 10 oz-in | _____ | dBm |
| 15 oz-in | _____ | dBm |
| 20 oz-in | _____ | dBm |
| 6. Third harmonic level with: | | |
| Unplated press fit center pin and sleeve | _____ | dBm |
| Gold plated press fit center pin and sleeve | _____ | dBm |
| Soldered center pin and sleeve | _____ | dBm |
| 7. Third harmonic level with pre-stressed soldered center pin
and sleeve | _____ | dBm |
| After resoldering outer sleeve (if necessary) | _____ | dBm |
| 8. Third harmonic level with prestressed gold plates press
fit center pin and sleeve | _____ | dBm |
| Third harmonic level after flow coating center
connection | _____ | dBm |
| 9. Third harmonic level before flow coating filter | _____ | dBm |
| Third harmonic level after flow coating filter | _____ | dBm |

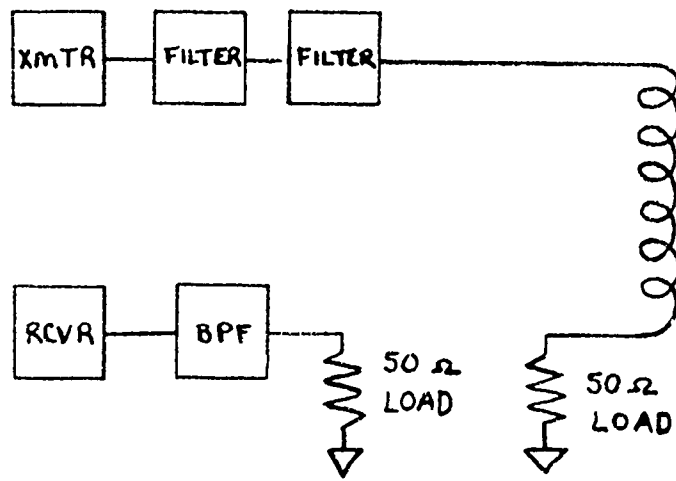


Figure E1

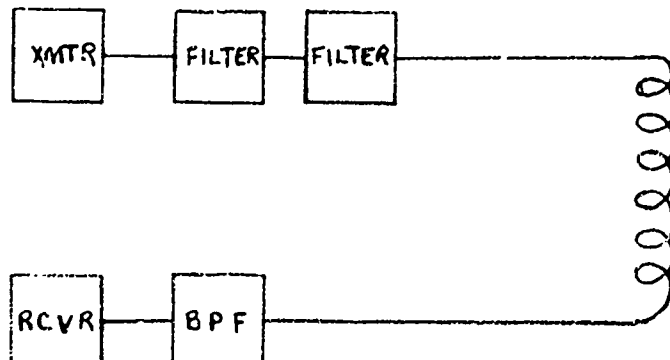
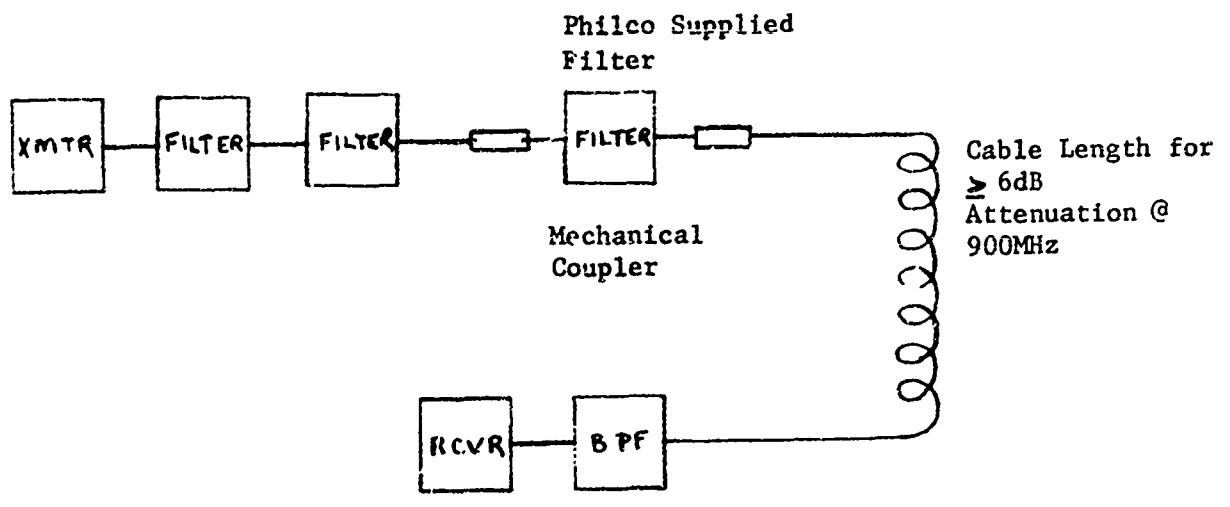
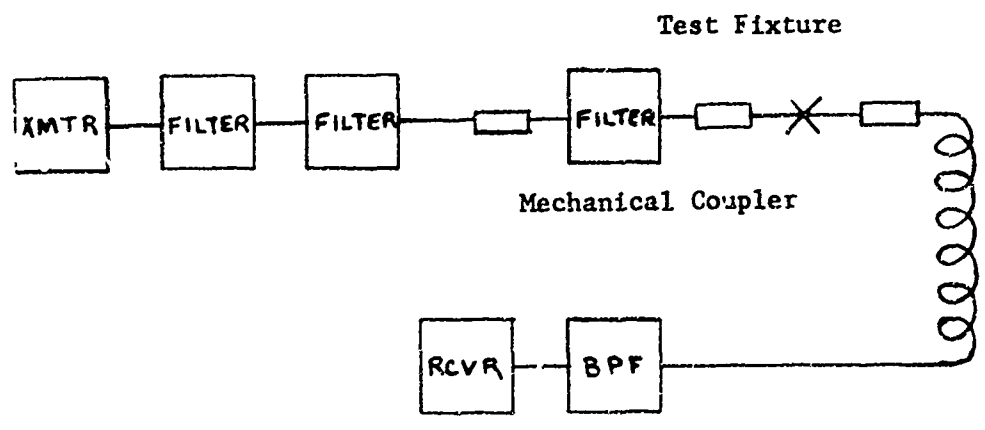


Figure E2

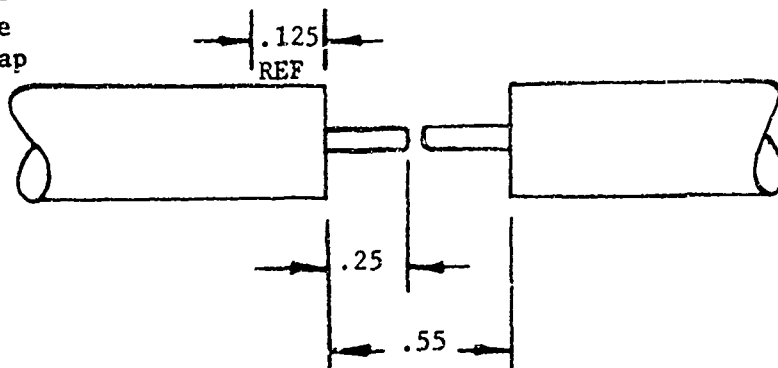


FigureE3



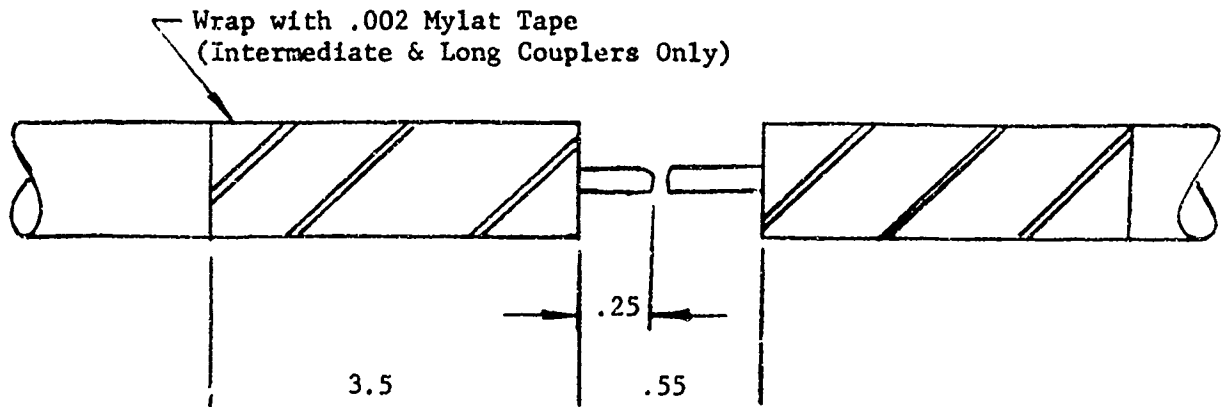
FigureE4

Solder
Sleeve
Overlap



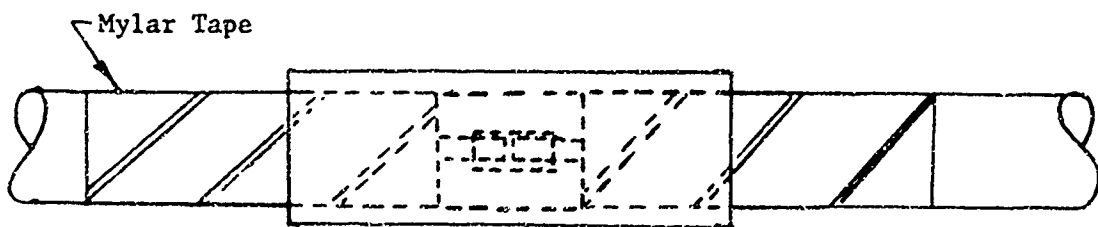
Cable Dimensions for
Soldered Connections

FigureE 5



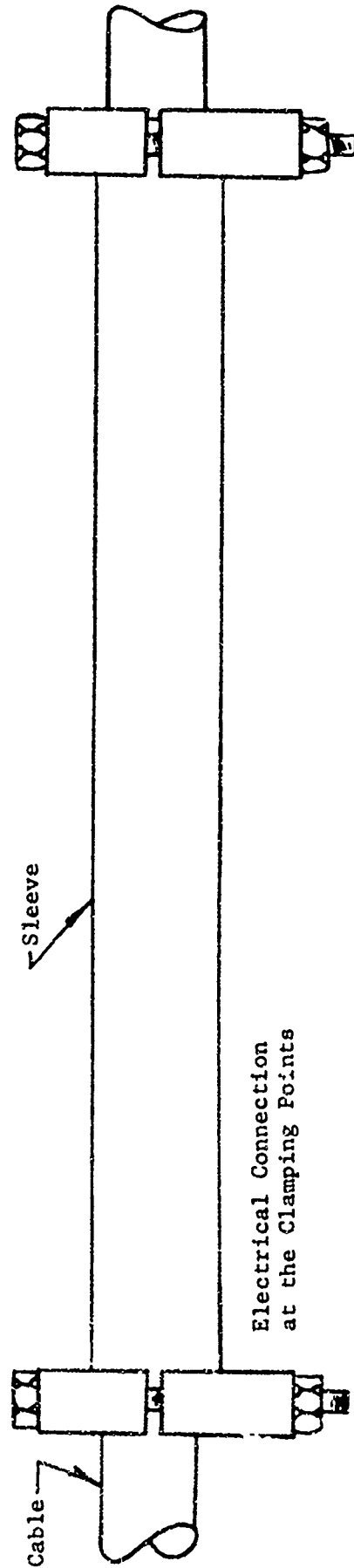
Preparation of Cable for Mechanical Couplers

Figure E6



Contactless (Intermediate Length) Mechanical Coupler

Figure E7



Assembled Cable and Coupler
(Short and Long Couplers Only)

FigureE8